

University of Windsor

Scholarship at UWindor

Electronic Theses and Dissertations

Theses, Dissertations, and Major Papers

11-8-2023

Exploring Paper as a Substrate for Printed Electronics

Lauren Jessica Renaud

University of Windsor

Follow this and additional works at: <https://scholar.uwindsor.ca/etd>

 Part of the [Chemistry Commons](#)

Recommended Citation

Renaud, Lauren Jessica, "Exploring Paper as a Substrate for Printed Electronics" (2023). *Electronic Theses and Dissertations*. 9202.

<https://scholar.uwindsor.ca/etd/9202>

This online database contains the full-text of PhD dissertations and Masters' theses of University of Windsor students from 1954 forward. These documents are made available for personal study and research purposes only, in accordance with the Canadian Copyright Act and the Creative Commons license—CC BY-NC-ND (Attribution, Non-Commercial, No Derivative Works). Under this license, works must always be attributed to the copyright holder (original author), cannot be used for any commercial purposes, and may not be altered. Any other use would require the permission of the copyright holder. Students may inquire about withdrawing their dissertation and/or thesis from this database. For additional inquiries, please contact the repository administrator via email (scholarship@uwindsor.ca) or by telephone at 519-253-3000ext. 3208.

Exploring Paper as a Substrate for Printed Electronics

By

Lauren J. Renaud

A Thesis
Submitted to the Faculty of Graduate Studies
through the Department of Chemistry and Biochemistry
in Partial Fulfillment of the Requirements for
the Degree of Master of Science
at the University of Windsor

Windsor, Ontario, Canada

2023

© 2023 Lauren J. Renaud

Exploring Paper as a Substrate for Printed Electronics

by

Lauren J. Renaud

APPROVED BY:

C. Semeniuk
Department of Integrative Biology

S. Rondeau-Gagne
Department of Chemistry and Biochemistry

T. Carmichael, Advisor
Department of Chemistry and Biochemistry

October 6, 2023

DECLARATION OF ORIGINALITY

I hereby certify that I am the sole author of this thesis and that no part of this thesis has been published or submitted for publication.

I certify that, to the best of my knowledge, my thesis does not infringe upon anyone's copyright nor violate any proprietary rights and that any ideas, techniques, quotations, or any other material from the work of other people included in my thesis, published or otherwise, are fully acknowledged in accordance with the standard referencing practices. Furthermore, to the extent that I have included copyrighted material that surpasses the bounds of fair dealing within the meaning of the Canada Copyright Act, I certify that I have obtained a written permission from the copyright owner(s) to include such material(s) in my thesis and have included copies of such copyright clearances to my appendix.

I declare that this is a true copy of my thesis, including any final revisions, as approved by my thesis committee and the Graduate Studies office, and that this thesis has not been submitted for a higher degree to any other University or Institution.

ABSTRACT

With the Internet of Things (IoT) rapid expansion the use of printed electronics that can be easily integrated into everyday life is gaining traction. These devices often use plastics as a substrate due to their flexibility; however, they are not biodegradable and contribute to our growing electronic waste (e-waste) problem. A greener alternative that is sought after is paper. Paper is biodegradable, flexible, and already familiar to many printing processes. Though paper appears smooth its surface is rough due to being composed of cellulose fibers which create pores. In the printed electronics (PE) industry, these pores are typically seen as a challenge, whereas we view this as an opportunity to learn more about how ink prints onto paper. Our work explores the wicking dynamics of silver nanowire (AgNW) ink into paper and how modifying the pore size can be taken advantage of for printing.

Chapter 2 describes the ability to select the optimal materials for printing electronic devices on paper by considering the desired performance for a specific application. AgNWs are highly sought after for printing functional inks for electronics because their entanglement offers inherent flexibility. They come in various aspect ratios and can be found in different concentrations of solutions. Paper comes in various pore sizes which can influence the conductivity and resolution of a functional ink. Investigating the interaction of the ink and substrate together, we show how the AgNW ink dimensions can be matched with the paper pore size. This chapter serves as a tool to help determine which parameters should be chosen based on the intended result for a printed device.

Chapter 3 expands on the findings of Chapter 2 by understanding that pore size has an effect on how inks penetrate the paper. With this knowledge, modifying the pore size through Debossed Contact Printing (DCP) allows for a patterned paper substrate. Debossing causes the pores to collapse creating indents in the paper that act as boundaries where ink is not able to wick through. Printing a conductive ink wherein the ink wets only the untouched pores creates a functional substrate. We then show that this can be used as a functional base to make a multilayer light-emitting paper device.

ACKNOWLEDGEMENTS

It is quite amazing how certain things come to be that you cannot picture it any other way. My research journey began after my first year of university and that is all thanks to Dr. Tricia Carmichael for allowing me the opportunity to be a part of the Carmichael Lab. I feel that I am in the best place for me to learn and grow. I am very grateful for your guidance throughout all these years and for truly creating a safe environment for all of us. Thank you to Steve Carmichael for always being so welcoming, supportive, and willing to share your experiences. I am grateful for all the laughs and knowledge.

The endless support from the Carmichael Lab, past and present, solidifies my decision to continue my chemistry education. I might be biased, but I do think our group is truly the best. Thank you for being there through the successes and the tears. I know I can count on you all to be in my corner. I look forward to our continued Greek Grill lunches, Swiss Chalet dinners, and our everyday shenanigans. I thank you all for your friendship and kindness, and for making the lab environment one that I'm excited about and proud to be a part of. I can't wait to see what we do in the future.

Thank you to Dr. Simon Rondeau-Gagne and Dr. Christina Semenuik for being on my committee and for always providing support and constructive feedback, making me a better chemist.

To my friends, old and new, who have grown with me and will continue to grow alongside me, thank you for your unwavering support. As you all follow your passions in different areas or even different cities, I appreciate you being able to weather even the most dangerous of storms with me. No matter how far out you go, you will always have a home with me.

And thank you to my family, including my cats Fanthom and Shadow, for being there through it all. For all the encouragement during dinner conversations and car rides, small reminders of my strength in post-it notes or a last-minute text message before a big presentation, and for always having my best interest in mind. To my cats for keeping me company as I studied and wrote. You are all the reason I reach for the stars.

TABLE OF CONTENTS

DECLARATION OF ORIGINALITY iii

ABSTRACT iv

ACKNOWLEDGEMENTS v

LIST OF TABLES viii

LIST OF FIGURES ix

LIST OF SUPPLEMENTARY TABLES xii

LIST OF SUPPLEMENTARY FIGURES xii

LIST OF ABBREVIATIONS/SYMBOLS xiii

CHAPTER 1 INTRODUCTION 1

 1.1 *Internet of Things* 2

 1.11 *Smart Packaging* 2

 1.2 *Printed Electronics* 4

 1.21 *Debossed Contact Printing* 5

 1.22 *Traditional Substrates for Printed Electronics* 6

 1.23 *Paper-based Printed Electronics* 8

 1.3 *Functional Inks* 13

 1.31 *Silver Inks* 15

 1.32 *Silver Nanowires* 16

 1.4 *Paper-based Printed Electronic Devices* 17

 1.41 *Alternating Current Electroluminescence (ACEL) Devices* 18

 1.5 *Scope of Thesis* 21

 1.6 *References* 22

CHAPTER 2 SYNCHRONIZING THE PORE SIZE OF PAPER SUBSTRATES
AND ASPECT RATIO OF SILVER NANOWIRES TO IMPROVE PRINTED
ELECTRONICS 31

 2.1 *Introduction* 32

2.2 <i>Results and Discussion</i>	34
2.3 <i>Conclusion</i>	46
2.4 <i>Experimental</i>	47
2.5 <i>References</i>	48
2.6 <i>Supporting Information</i>	52
CHAPTER 3 LIGHT-EMITTING PAPER FABRICATED USING DEBOSSSED CONTACT PRINTING	53
3.1 <i>Introduction</i>	54
3.2 <i>Results and Discussion</i>	57
3.3 <i>Conclusion</i>	62
3.4 <i>Experimental</i>	63
3.5 <i>References</i>	64
3.6 <i>Supporting Information</i>	66
CHAPTER 4 CONCLUSION AND OUTLOOK	68
APPENDICES	70
VITA AUCTORIS	76

LIST OF TABLES

Table 2.1 Sheet resistance values in relation to concentration and pore size for a) AgNW30 and b) AgNW200.....43

LIST OF FIGURES

Figure 1.1 Johnnie Walker Blue Label with incorporated electronic tag that is connected to the IoT a) shows the seamless integration into the product, b) the electrical component becomes exposed once opening the bottle, c) NFC lets consumers interact with the product using NFC-enabled smartphones.....	3
Figure 1.2 Schematic breaking down the different printing technologies used in printed electronic processes.....	5
Figure 1.3 DCP schematic illustrating the fabrication process to achieving a functionalized substrate.....	6
Figure 1.4 Examples of flexible devices on plastic substrates a) touch sensor printed onto a PET substrate, b) PI substrate with functional organic TFTs and organic complementary circuits	7
Figure 1.5 Schematic of global production, use, and fate of polymer resins, synthetic fibers, and additives with majority of waste being discarded or incinerated.....	8
Figure 1.6 Nanostructured paper prepared from wood chips; a) an image of spruce wood chips, b) Scanning Electron Microscopy (SEM) image of purified cellulose pulp fibres, c) SEM image of cellulose nanofibres after mechanical nanofibrillation, d) image of nanostructured paper and e) SEM image of its casting surface, and f) SEM image of silver nanoparticle ink.....	9
Figure 1.7 SEM images of the top-view (left) and cross section (right) of paper after inkjet printing a) one layer and b) three layers of silver on chromatography paper.....	11
Figure 1.8 Scanning electron microscopy (SEM) images of silver nanowires at two magnifications.....	17
Figure 1.9 A stretchable ACEL fiber where a) shows the schematic of the device, b) Photographs show the original shape of the device (left) and when the fiber is	

subjected to a stretched strain of 80% (right), and c) Photograph of the knotted ACEL device.....19

Figure 1.10 Schematics of ACELs with a) the symmetric and b) the asymmetric configurations, respectively.....20

Figure 2.1 SEM characterization at 1500x magnification of filter paper of pore sizes a) 2.5 μm b) 8 μm c) 11 μm and d) 20-25 μm35

Figure 2.2 Still images of 10 μL of 3 mg/mL AgNW30 solution in ethanol at zero, six and twelve seconds after deposition on filter paper of pore size a) 2.5 μm and b) 20-25 μm36

Figure 2.3 Still images of 10 μL of 3 mg/mL AgNW200 solution in ethanol at zero, six, and twelve seconds on filter paper of pore size a) 2.5 μm and b) 20-25 μm36

Figure 2.4 Maximum lateral wicking diameter over time for the AgNW front for a) AgNW30 b) AgNW200.....37

Figure 2.5 Cross-sectional SEM of 3 mg/mL AgNW solutions deposited on filter paper of at 2.5 μm , 8 μm , 11 μm and, 20-25 μm at 600x magnification a) AgNW30 b) AgNW200.....38

Figure 2.6 SEM characterization at 1500x magnification of AgNW30 solution on filter paper with pore sizes of 2.5 μm , 8 μm , 11 μm , and 20-25 μm at concentrations of a) 3 mg/mL b) 2 mg/mL c) 0.7 mg/mL and d) 0.4 mg/mL.....39

Figure 2.7 SEM characterization at 1500x magnification of AgNW200 solution on filter paper with pore sizes of 2.5 μm , 8 μm , 11 μm , and 20-25 μm at concentrations of a) 3 mg/mL b) 2 mg/mL c) 0.7 mg/mL and d) 0.4 mg/mL.....40

Figure 2.8 SEM characterization of the edge of the AgNW30 front on filter paper with pore size 2.5 μm , 8 μm , 11 μm , and 20-25 μm at concentrations of a) 0.4 mg/mL and b) 3 mg/mL.....41

Figure 2.9 SEM characterization of the edge of the AgNW200 front on filter paper with pore size 2.5 μm and 20-25 μm at concentrations of a) 0.4 mg/mL and b) 3 mg/mL.....	42
Figure 2.10 Sheet resistance of a) AgNW30 and b) AgNW200 in relation to concentration and pore sizes of 2.5 μm (blue), 8 μm (red), 11 μm (green), and 20-25 μm (purple).....	43
Figure 2.11 Sheet resistance in relation to pore sizes for 0.4 mg/mL solution (blue) and 0.7 mg/mL solution (orange) for a) AgNW30 and b) AgNW200.....	44
Figure 2.12 Change in resistance during bending of 3 mg/mL AgNW30 on filter paper of pore size a) 20-25 μm b) 11 μm c) 8 μm d) 2.5 μm	45
Figure 2.13 Change in resistance during bending of 3 mg/mL of a) AgNW30 and b) AgNW200 on filter paper of pore size 2.5 μm	46
Figure 3.1 Schematic of paper-based ACEL fabrication.....	58
Figure 3.2 Picture of debossed pattern on a paper substrate.....	59
Figure 3.3 a) Microscope image of one coat of silver ink on paper, b) Microscope image of two coats of silver ink on paper, c) Microscope image of barium titanate mixed with PDMS layer d) Microscope image of copper doped zinc sulfide mixed with PDMS layer, e) Microscope image of 2 coats of PEDOT: PSS printed on top of PDMS, f) Microscope image of 2 coats of PEDOT: PSS printed on top of NOA-73.....	60
Figure 3.4 Photograph of the completed ACEL device with copper tape as bottom and top contact.....	62
Figure 3.5 Photograph of three ACEL devices when subjected to AC voltage....	62

LIST OF SUPPLEMENTARY TABLES

Table S2.1 Drop diameter value for the AgNW front of a) AgNW30 and b) AgNW200.....52

LIST OF SUPPLEMENTARY FIGURES

Figure S3.1 Microscope images of the dielectric layer when a) spincoated, and b) roller printed.....66

Figure S3.2 Microscope images of the emissive layer with a) no dielectric layer, and b) with barium titanate as the dielectric layer.....67

LIST OF ABBREVIATIONS/SYMBOLS

~	approximately
≈	almost equal to
°	degree
AC	Alternating Current
ACEL	Alternating Current Electroluminescence
AgNW	silver nanowires
CNT	carbon nanotubes
DCP	Debossed Contact Printing
Hz	hertz
g	grams
kg	kilograms
m	meter
IoT	Internet of Things
e-waste	Electronic Waste
LED	Light Emitting Diode
LEEC	Light Emitting Electrochemical Cell
OLED	Organic Light Emitting Device
MOD	Metal-Organic Decomposition
NCP	Nanocellulose Paper
NFC	Near Field Communication
PE	Printed Electronics
PEDOT: PSS	poly-3,4-ethylenedioxythiophene poly-styrene sulfonate
PDMS	polydimethylsiloxane
RFID	Radio Frequency Identification

SEM	Scanning Electron Microscopy
PET	polyethylene terephthalate
PI	polyimide
TFT	Thin Film Transistor
μ	micro
n	nano
dm	decimeter
cm	centimeter
mm	millimeter
UV	ultraviolet
V	volts

CHAPTER 1
INTRODUCTION

1.1 Internet of Things

In the era of digital advancement, the Internet of Things (IoT) has emerged as a paradigm-shifting phenomenon that is reshaping the way we perceive, interact with, and manage the world around us. The IoT is a vast information system that connects a multitude of smart sensors, devices, and systems for data collection and exchange.¹ The IoT has already been integrated into many sectors and encompasses fields from healthcare and transportation to agriculture and urban planning.¹ The IoT is driven by an expansion of the Internet through the inclusion of physical objects combined with an ability to provide smarter services to the environment as more data becomes available².

Advancing technology allows for information to be shared quicker, more efficiently, and to reach a higher volume of people. As sensor technology, data processing capabilities, and wireless connectivity continue to evolve, the IoT works to make sharing information more seamless and for the data collected to give added benefits to consumers.^{1,3} The ability of these devices to collect, transmit, and analyze data in real-time opens up unique opportunities for optimizing processes, enhancing decision-making, and decreasing human error while permitting new forms of human-machine interaction.^{1,2} This connectivity of the information drives a need for better devices that are portable, flexible, lightweight and have good performance.⁴

The IoT is a useful innovation that has the potential to improve the quality of life in all aspects of life: professional, personal, and social environments.² It facilitates access to specific information and services to create a safer, healthier, and more fulfilling environment.^{1,5,6}

1.11 Smart Packaging

As part of the growing IoT, the smart packaging industry has really developed. Smart packaging combines active and intelligent packaging: two innovative approaches to improving the food and packaging industries.⁷ Active packaging monitors the environment of the product, where components may add or absorb substances into the environment or package to counteract unwanted conditions and improve shelf life.^{7,8} Intelligent packaging monitors the quality of the contents itself and can track and relay this information.^{7,9}

Smart packaging refers to packaging systems that have devices embedded to gain information about foods, pharmaceuticals, cosmetics, and other perishable goods, as well as the state of the environment during storage and transport.^{8,9} According to Schaefer and Cheung (2018), smart packaging is used to extend shelf life, monitor freshness, display information on quality, and improve product and consumer safety.⁸ Some of these devices include antennas^{7,9,10}, displays^{7,11}, and sensors^{7-9,12,13} that monitor aspects such as food quality, temperature, gas levels, and damage to the package.

An example of this is when the liquor company Diageo teamed up with ThinFilm and used an electronically tagged bottle for their Johnnie Walker Blue Label Whisky as seen in Figure 1.1.¹⁴ The bottle uses near field communication (NFC) to let consumers interact with the package using their NFC-enabled smartphones. The aim was to enrich the consumers experience by sharing relevant information such as cocktail recipes and promotional content while ensuring a top-quality product.¹⁴



Figure 1.1 Johnnie Walker Blue Label with incorporated electronic tag that is connected to the IoT a) shows the seamless integration into the product, b) the electrical component becomes exposed once opening the bottle, c) NFC lets consumers interact with the product using NFC-enabled smartphones.

Another example is the approach of looking at carbon monoxide levels as the package is being transported to the consumer. A review done by Puligundla et al. (2012) looked at the importance of incorporating a carbon monoxide sensor in food products.¹³ To keep microbial growth at bay some food products are packed under an environment of

complete or near complete carbon dioxide atmosphere. A sensor that monitors carbon dioxide could indicate when there is a drop in carbon dioxide levels due to a leakage, giving insight into the product quality and indicating the freshness.

Overall, smart packaging offers an added benefit to regular packaging, wherein information about the condition of the contents at each stage of its journey from manufacturer to consumer can be monitored. The idea of smart packaging is advantageous as we become more aware of human health and more involved in the products we consume, opting for products that are minimally processed and easily prepared.¹³

IDTechEx estimates that the global market for electronic smart packaging will reach a value of US\$2.6 billion in 2033.¹⁵ In order to keep up with the volume demanded by this market growth, these smart packages will require devices and sensors that are fabricated by high-throughput printing methods.¹⁶ This results in the packaging industry turning to printed electronics (PE) to continue building these devices in order to keep packaging technology moving forward.

1.2 Printed Electronics

The basis of printed electronics works to integrate devices and create electronic components on different substrates through various traditional printing methods by patterning conductive, semi-conductive, and insulating materials.^{17,18} This field of work tends to be very innovative wherein it strives to create electric devices and circuits that are flexible, lightweight, and made with cost-effective materials.⁴

The printing processes used in PE allow for the rapid and scalable production of devices, making it possible to manufacture electronics in large quantities at relatively low costs.¹⁸ As shown in Figure 1.2 the printing methods used in PE can be split into two categories: contact printing and non-contact printing.⁴ With contact printing, the patterned structures of the printing method are coated with ink and come into physical contact with the substrate.⁴ An example is flexographic printing.¹⁹ In non-contact printing, such as inkjet, the ink is dispensed by an opening and the structures are defined

by moving the stage holding the substrate in order to create the pre-determined pattern.⁴ Inkjet printing uses nozzles to eject the ink at a distance away from the substrate.²⁰

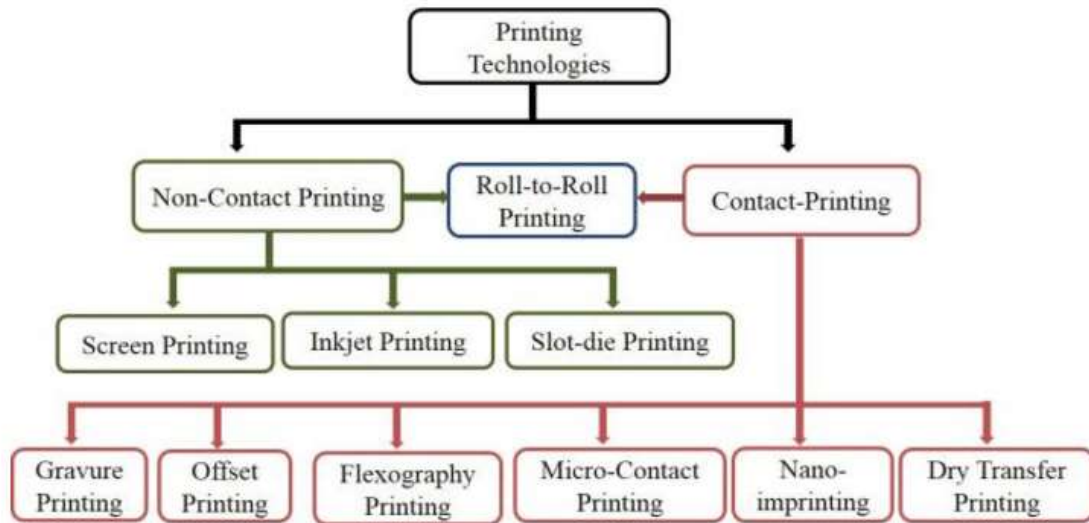


Figure 1.2 Schematic breaking down the different printing technologies used in printed electronic processes. Reproduced with permission from Creative Commons for reference [4].

With the existing printing processes, there are certain conditions that make each method beneficial and give the optimal product.¹⁸ Trying to figure out these parameters can take many attempts. Sometimes it can be difficult to find compatibility between the ink and the substrate.²¹ Different methods need different ink conditions, having to tune the viscosity or surface tension, limiting the application to which printing process can be used.^{4,20} With contact printing involving rollers or stencils, separate rollers or resists may be needed to print more than one pattern. Certain printing processes take multiple steps which can be time consuming in production or ensuring good quality printing passes and can also waste a lot of material.

1.21 Debossed Contact Printing

Debossed Contact Printing (DCP) is a new printing method designed for porous substrates created by the Carmichael Lab as an alternative to other roller involved printing techniques that require a patterned roller or resists.²² It works by taking advantage of the compressibility of the porous structure of a substrate, such as paper, and modifying the size of the pores by applying pressure using a debossing tip. This pressure causes the pores to collapse into a selected relief pattern and lowers these regions away

from the contact plane. As demonstrated in Figure 1.3, the raised, uncompressed portion of the substrate gets coated with ink through contact with a roller. This method has been demonstrated on paper substrates with silver ink, carbon black ink, and poly-3,4-ethylenedioxythiophene poly-styrene sulfonate (PEDOT:PSS) ink.

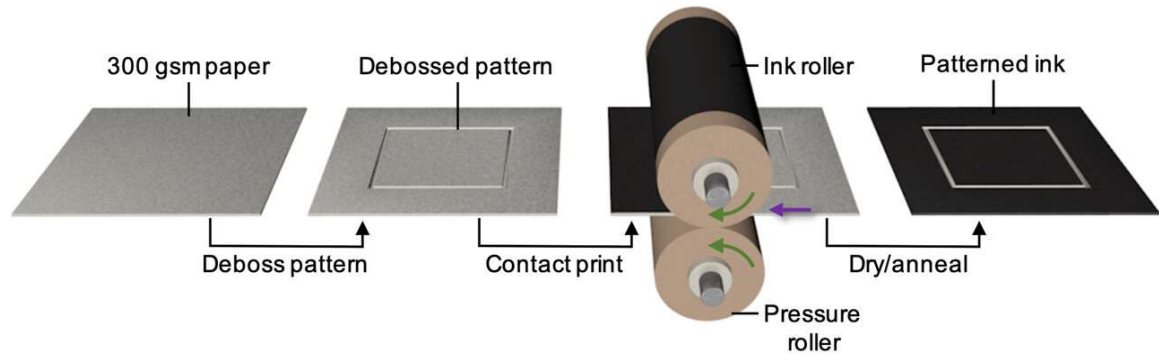


Figure 1.3. DCP schematic illustrating the fabrication process to achieving a functionalized substrate. Reproduced with permission from Copyright Clearance Centre RightsLink for reference [22].

1.22 Traditional Substrates for Printed Electronics

Traditional substrates that are used in PE are silicon or plastics. With electronics moving away from rigid structures and toward having devices be more conformable to softer shapes, such as packaging that take on arbitrary shapes, flexible and stretchable substrates are the foundation to meeting those requirements. Figure 1.4 shows examples of devices printed on plastics.^{23,24} Figure 1.4a is screen printed touch sensor on a polyethylene terephthalate (PET) substrate and Figure 1.4b is a thin flexible transistor (TFT) on a polyimide (PI) substrate. The substrate of choice is typically plastic, mainly PET is used due to its smoothness, flexibility, and low cost.^{9,25}

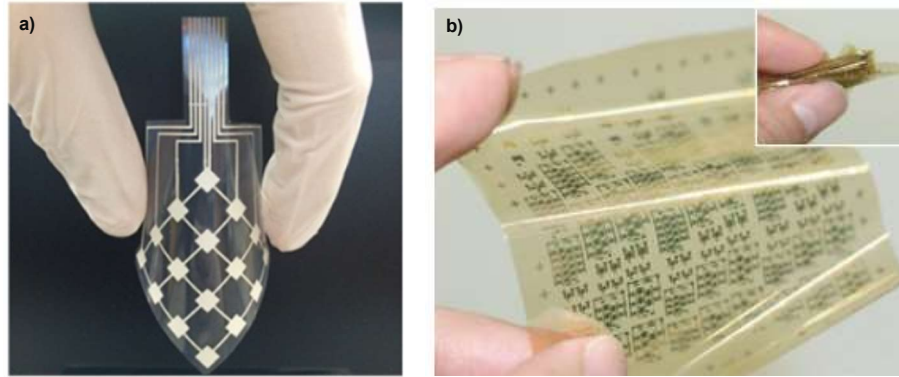


Figure 1.4 Examples of flexible devices on plastic substrates a) touch sensor printed onto a PET substrate, b) PI substrate with functional organic TFTs and organic complementary circuits. Reproduced with permission from Copyright Clearance Centre RightsLink for reference [23,24].

Printing on a planar substrate like PET allows for two distinct layers to be formed: the substrate and a thin film of ink. The ink is able to spread along the smooth surface and form a uniform layer. However, PET along with other plastics are not biodegradable and will have to be recycled once its use is done.

With IoT expanding, the use of these substrates will exacerbate the on-going electronic waste (e-waste) problem. When electronics are at the end of their life cycle, the bulk of the device determines which recycle stream they are disposed in. For most printed electronics, the substrate is plastic where they are disposed of in landfills and accumulate. Figure 1.5 depicts the cycle, or lack of cycle, when it comes to dealing with e-waste.²⁶ Eventually these plastics migrate into aquatic environments and contaminate the ecosystem.^{26,27} The leftover technology itself is considered harmful to the environment and human health but to aid in the disposal toxic solvents are used, making it an even bigger issue.

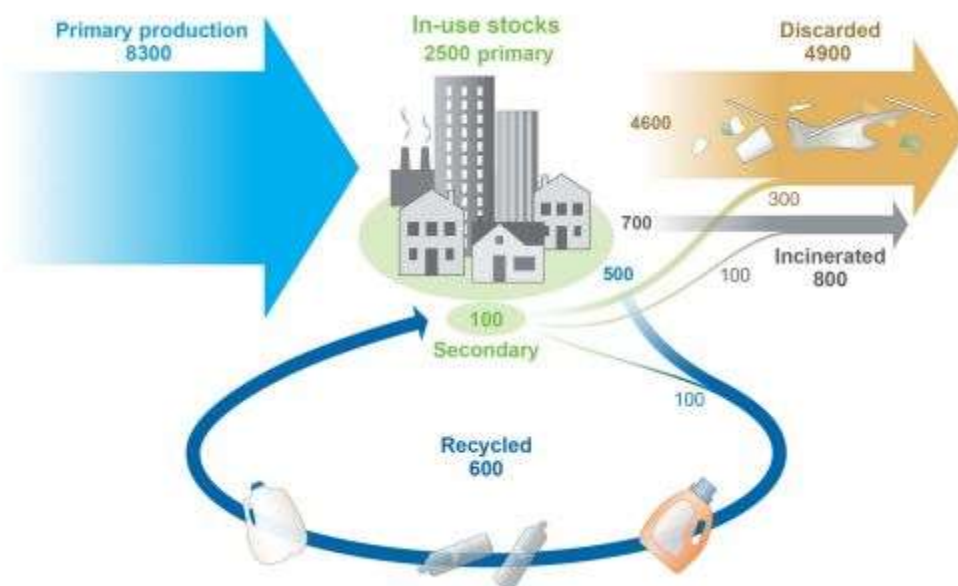


Figure 1.5 Schematic of global production, use, and fate of polymer resins, synthetic fibers, and additives with majority of waste being discarded or incinerated. Reproduced with permission from Creative Commons for reference [26].

Canada does not have any national legislation regarding e-waste and though there are recycling programs and agencies the tracking of all the waste generated is scarce.²⁸ It has been found that both illegal exportation and inappropriate donation of electronic equipment from developed to developing countries takes place.²⁹ In Canada, the e-waste generation per capita was found to be 25.3 kg in 2020 and is estimated to rise to 31.5 kg in the next ten years.²⁸ With the illegal transport and lack of tracking, Canada is merely putting the burden of the damage that will come onto other countries and is not being held fully responsible for our e-waste footprint. With this startling increase in e-waste and as the demand for electronics to be integrated into product packaging will continue to rise, the need to move away from plastics as a substrate and towards devices that use green materials, such as paper, becomes even more evident.

1.23 Paper-based Printed Electronics

With the ideology to shift focus from harmful materials, paper-based electronics involves the integration of electronic devices and circuits on paper substrates using different fabrication techniques. Devices that have been successful with a paper substrate include transistors, diodes, sensors, energy storage devices, and more.¹⁸ This emerging

field of research has the potential to change the way we interact with technology, by enabling the creation of low-cost, lightweight, and environmentally friendly electronic devices while being robust and scalable.³⁰

Paper is abundant, renewable, biodegradable, and recyclable, making it an ideal material for sustainable and green electronics. Moreover, paper is lightweight and flexible, which makes it suitable for applications where weight and flexibility are important, such as wearable electronics, sensors, and smart packaging. Another benefit is it is more cost effective than traditional substrates, costing ≈ 0.1 cent dm^{-2} as compared to PET being ≈ 2 cent dm^{-2} and polyimide being ≈ 30 cent dm^{-2} .¹⁸ In addition, paper is versatile and already familiar in many printing processes¹⁹ and often can withstand higher processing temperatures than plastics.^{18,19}

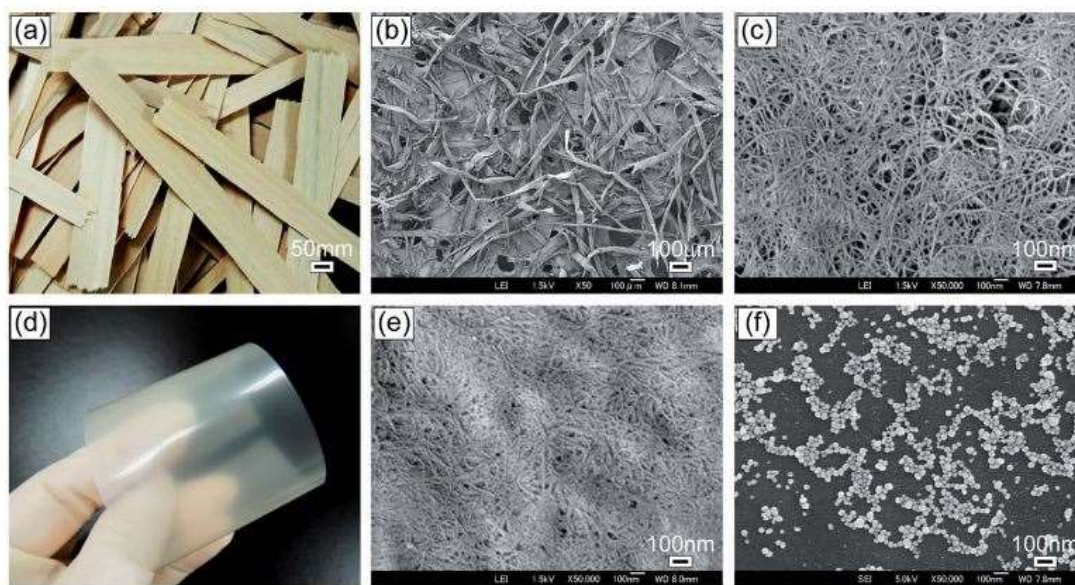


Figure 1.6 Nanostructured paper prepared from wood chips; a) an image of spruce wood chips, b) Scanning Electron Microscopy (SEM) image of purified cellulose pulp fibres, c) SEM image of cellulose nanofibres after mechanical nanofibrillation, d) image of nanostructured paper and e) SEM image of its casting surface, and f) SEM image of silver nanoparticle ink. Reproduced with permission from Copyright Clearance Centre Marketplace for reference [31].

Paper is made by first dewatering a dilute suspension of cellulose fibers taken from wood or plants and then undergoing a filtration process creating a pulp. Figure 1.6a is an example of wood as a starting material to create paper products.³¹ The pulp is pressed and

heated resulting in the finished product known as paper.^{18,32,33} There are many different classifications of paper which can vary based on grammage and additives. This can impart microstructural differences to the pore network, as outlined in Figure 1.6b-f,³¹ giving different types of paper different properties such as strength, brightness, drying rate, burn rate, and more.^{33,34}

Grammage refers to the mass per unit area for a paper sheet.^{18,34} Typical paper is around 80 g per m² with a thickness of 100 μm and can range anywhere up to around 800 g per m². Paper that is heavier than 200 g per m² and has a thickness of 300 μm is referred to as paperboard or cardboard.¹⁸ To functionalize the paper many different additives can be included into the pulp before it is pressed and dried. This can include binders, sizing agents, coating aids, strength agents, optical brighteners, and more.³⁵ Binders such as chalks, clays, and talcs are added to modify surface smoothness and ink absorbency.^{18,36} Calcium carbonate falls under a chalk binder classification and is a common additive in many papers. Sizing agents are one of the most common additives in everyday paper products such as packaging of food products and paper cups.³⁵ Starches, gum, and rosin fall under this category and work to increase mechanical strength and hydrophobicity.^{18,35}

Paper is composed of a fibrous structure of cellulose. These cellulose fibers are micro-fibril bundles that can be tens of millimeters long that form a pore network.³³ The structure of paper results in a rough, porous, and hydrophilic surface. The hydroxyl groups of the cellulose fibers promotes the absorption of ink through the pores and into the paper upon deposition.^{37,38} The porosity and hydrophilicity of paper becomes a challenge in printing due to capillary wicking.³³ The fibrous structure of paper gets in the way of the ink and reduces the ability to print sharp features.³⁹ Figure 1.7 shows a SEM image top-view when silver nanowires (AgNWs) are printed on paper that the ink experiences lateral and vertical wicking.⁴⁰ The ink also penetrates the surface and wicks down into the substrate, creating a composite,^{41,42} as seen in the cross-sectional images of Figure 1.7.⁴⁰ Ink bleeding occurs when the ink diffuses past its desired boundary. This has a larger impact when printing active inks as the pores disrupt the active networks

causing them to become 3D instead of planar and will further affect electrical properties by increasing resistance.³⁹

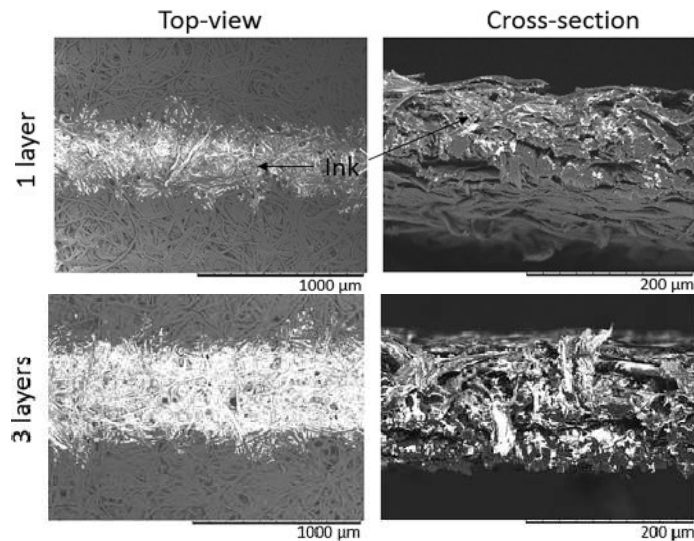


Figure 1.7 SEM images of the top-view (left) and cross section (right) of paper after inkjet printing a) one layer and b) three layers of silver on chromatography paper. Adapted with permission from Copyright Clearance Centre RightsLink for reference [40].

As previously mentioned, paper is rough, porous, and hydrophilic which can negatively affect printing. There are multiple ways to combat these perceived disadvantages and is often taken from the perspective of surface tuning in order to get the desired printing resolution. To combat the wicking of inks into paper, modification to the paper itself to make the surface more hydrophobic has been investigated. This can be done by changing the composition of the paper.^{38,43} Ahn et al. (2020), removed the calcium carbonate fillers of an A4 paper through acid treatment and replaced it with alkoxide functional groups.³⁸ This was followed by modification steps to end up with chloro-silane based fillers which altered the pore size of the paper. This modification would lessen the wicking and improve printing resolution.³⁸

Another popular approach is to hide the rough topographical landscape of paper under a coating or resin to planarize the surface.^{19,44,45} Materials such as polymers, epoxy, latex, etc. will fill the pores and cover the surface making it smooth and flat, improving the resolution and electrical performance of the conductive inks. Jansson et al. (2022) compared flexographically printed silver nanoink on uncoated and coated papers.¹⁹ Their

study showed that ink absorbs into the pores of uncoated paper, resulting in surface irregularities and an inability to attain uniformity on rougher paper substrates. In contrast, the coated paper has a planarized surface, providing comparable ink uniformity, printing resolution, and sheet resistance as that printed on PET.¹⁹

A third approach is patterning hydrophobic resists on the substrate so when an ink is deposited it only wets the parts that are left unmasked and are hydrophilic.⁴⁶

These methods have provided effective functionality for printing; however, there is concern about the environmental effects of the coatings and modifications, as well as the impact on the recyclability and biodegradability of the paper substrate. Polymer or wax coatings such as polyethylene, PET, or paraffin wax once layered onto the paper weakens the composability, therefore undoing the notion of moving towards green materials.⁴⁷

Though the porosity and hydrophilicity of paper can make printing more challenging, there are benefits to having a porous substrate. There is improved adhesion of thin films onto the substrate and binding of materials through mechanical interlock^{42,48} which becomes even more important on a device that will be bent or folded. The embedding of the ink inside the substrate prevents abrasion, crack formation, and chemical corrosion.^{31,42} The pores enhance the carrier transport efficiency and have microfluidic properties.^{33,44} Depending on the pore size of the paper absorption along the fibers upon deposition can keep material at the surface³¹ as opposed to wicking vertically as previously mentioned. The pores perpendicular to the surface of deposition entrap the inks in the pores and prevent lateral spread.²¹

With paper gaining more traction as a green substrate, there is a need to understand how to optimally functionalize it. Fabrication techniques that paper has shown compatibility with range from printing and coating to patterning and cutting, and they are being continuously improved to achieve better performance and functionality. The current and potential applications of paper-based electronics are diverse and include areas such as healthcare, food packaging, environmental monitoring, and energy storage.^{18,33,49} One possibility that has already been explored is paper-based sensors that could be used

for detecting food spoilage,^{10,13} monitoring humidity,^{18,33,43} or measuring vital signs in patients.³³

Understanding the substrate is half the battle, but to then take this porous substrate and create a device requires investigation into the functional material.

1.3 Functional Inks

An important component in the printing process is the ink being deposited. There is a lack of research surrounding how the substrate impacts the printability of the ink. With printing, various parameters need to be considered when looking for the right ink to match the substrate. The ink needs to be compatible with the substrate to have good adhesion and printability to result in clear resolution and perform for its intended use.⁵⁰

Breaking it down to the basics of an ink, there are usually two components: a liquid vehicle and dispersed component.⁵¹ The liquid vehicle is either water or an organic solvent and determines the properties of the ink.^{51,52} The dispersed component determines the functionality of the ink.^{50,51} Typically in printed electronics functional inks are composed of pigments, polymers, solvents, and additives.^{17,39,52} Polymers are added as a stabilizing/capping agent to give good dispersion and avoid agglomeration.^{50,52} Certain printing processes, such as inkjet, requires the use of a binder, typically a resin, to provide adhesion between the ink and the substrate.⁵⁰ With functional inks used for conductive electronics these pigments are replaced with metal particles, giving them conductivity.^{17,52,53}

Active inks include organic polymers, graphene⁵³, metal-organic decomposition (MOD)⁵⁴, nanotubes⁵³, nanoparticles, and nanowires. The conductivity of polymers is nowhere near that of metals^{42,52} and a major requirement is being able to print and keep the active networks.^{39,42} MODs require an extra post-treatment step to make them conductive, which involves heating to remove the organic ligands.⁵⁴ Paper substrates may not be able to tolerate the high temperatures required for this step. Carbon based inks such as graphene and carbon nanotubes (CNTs) have high electrical conductivity, high mechanical strength, optical transparency, and simple preparation. Metal inks still outperform these carbon-based inks and the downfall is that toxic solvents are required to

disperse the carbon component.^{42,53,55} Graphene and CNTs do not disperse well into solutions or liquids due to their van der Waals interaction keeping them agglomerated.⁵⁵

Metal loading is a crucial factor in printing conductive inks. In active inks metals are considered the fillers of the ink. Depending on how much filler is present in the ink will determine if the ink is conductive. With a higher metal loading there are more metal particles present. The closer the particles are within the ink the more likely they are able to create a conductive pathway. This is known as the percolation threshold which indicates how much filler is needed to get the ink to the point of conductivity.⁵² Each metal nanoparticle will require a different metal loading to reach its percolation threshold and with some printing processes multiple printing passes are needed to achieve conductivity.

Though metals are not considered “green materials”, they are still desired in electronic devices as they are needed for performance. In the overall design of the devices, metals make up a small amount in comparison to the substrate. This amount can be further minimized by choosing an ink that requires a smaller percolation threshold and fewer passes. Though it is important not to minimize the impact that metals have on the recyclability of PE, there are studies being done on reclaiming the metal and quantifying how much is returned.¹⁸

Ink formulation is a complex process. Besides the actual composition of the ink there are other characteristics that come into play when it comes to printability. Viscosity, surface tension, and wettability of the ink are all factors that will affect the print quality.¹⁷ These factors influence the drop size, drop placement accuracy, satellite formation, and wetting of the substrate.⁵⁰ Tuning the viscosity and surface tension of inks is a critical aspect when considering their application in various printing methods. Each printing technique, whether it's inkjet, screen printing, flexographic printing, or others, operates under distinct physical principles, necessitating tailored ink properties to achieve optimal results.^{17,20,42,52}

Inkjet printing requires inks with lower viscosity and surface tension values for droplet ejection.¹⁷ A well-adjusted ink viscosity ensures that droplets form consistently

and maintain their shape during flight, resulting in accurate placement on the substrate. Surface tension impacts droplet formation at the nozzle and the way droplets spread upon contact with the substrate. In this case, tuning the surface tension is needed to achieve uniform droplet size and prevent splattering or coalescence. Similarly, in screen printing, where ink is forced through a stencil onto the substrate, a higher ink viscosity is desired to ensure smooth and consistent ink flow.¹⁷ This allows for well-defined patterns to be deposited on the substrate. At the same time, reduced surface energies will reduce the wettability resulting in better line resolution.⁴ If the surface tension of the substrate is lower than the surface energy of the inks, good resolution can be achieved with low viscosity inks.⁴ Flexographic printing requires inks with specific rheological properties to accommodate the fine details of the printing plate and the continuous printing process. Tuning the ink viscosity is essential to achieving the right balance between flow and resistance, enabling the ink to transfer smoothly from the printing plate to the substrate. In addition, controlling surface tension is important for optimal wetting and ink transfer across the printing plate. Flexography requires lower viscosity and surface tension values than screen printing.⁵²

1.31 Silver Inks

Silver's electronic structure comprises a single valence electron that readily moves within its lattice and grants it the highest electrical conductivity among all metals.^{50,54,56} This high conductivity positions silver as a prime candidate for fabricating electronic components on PE substrates. In addition, silver offers distinct advantages over other metals commonly considered for similar applications. It is considered more cost-effective than gold and while copper is lower cost than silver, copper suffers from corrosion.^{20,50,53} Its compatibility with diverse printing techniques, prominently including inkjet and screen printing, allows for the creation of intricate circuits and conductive patterns with precision, making silver a promising choice for PE.

The adhesion of silver ink to various substrates enhances its versatility.⁵⁷, enabling its use on surfaces ranging from flexible polymers to traditional paper. This property, combined with its low sintering temperature, makes it particularly well-suited for integration with substrates sensitive to high temperatures⁵⁷. Silver's pervasive presence in

everyday wear, often found in jewelry, highlights its familiarity and usability across industries. Silver ink, available in forms such as flakes⁵⁰, nanoparticles^{50,51}, and nanowires⁵⁶, further amplifies its adaptability to different printing methods and design requirements. These different structures cater to specific needs, facilitating tailored solutions in PE device fabrication. Overall, silver ink's multifaceted characteristics, encompassing conductivity, compatibility, versatility, and various ink forms, position it as a driving force in the advancement of printed electronics across an array of innovative applications.

1.32 Silver Nanowires

Silver nanowires (AgNWs) represent one morphology of nanostructured inks available in the printing world. Typically synthesized using a polyol method, AgNWs are considered easily made and are commercially available.⁵⁸ The aspect ratio that can be achieved are a length between 20 μm to 200 μm with the diameter being between 20 nm to 100 nm.^{59,60} Nanowires can be suspended in solutions for depositions and are compatible with a range of solvents which enhances their versatility in applications. Upon drying, AgNWs establish an active network that can remain transparent⁵⁸ while still maintaining high electrical conductivity, which outperforms other inks. The network will lose its transparency with increasing concentration. Annealing, a post-process treatment, facilitates the sintering of junctions between metal particles, further enhancing their electrical conductivity.⁵⁴ Most often with AgNWs annealing is done thermally, where elevated temperatures allow the AgNWs to become more connected.⁶¹

AgNWs are often highly sought after for flexible printed electronics as they offer entanglement, which imparts flexibility to their structure. Figure 1.8 clearly visualizes this entanglement with the AgNWs overlapping repeatedly.⁵⁸ As mentioned above, AgNWs are available in various dimensions that range in both length and diameter. Longer NWs due to their aspect ratio exhibit more entanglement offering better conductivity⁵⁸, since the AgNWs have more points of connection within the electrical network. AgNWs aspect ratio sets them apart from other nanostructured inks, which require higher particle loading to achieve comparable performance, thereby consuming more material.⁵²

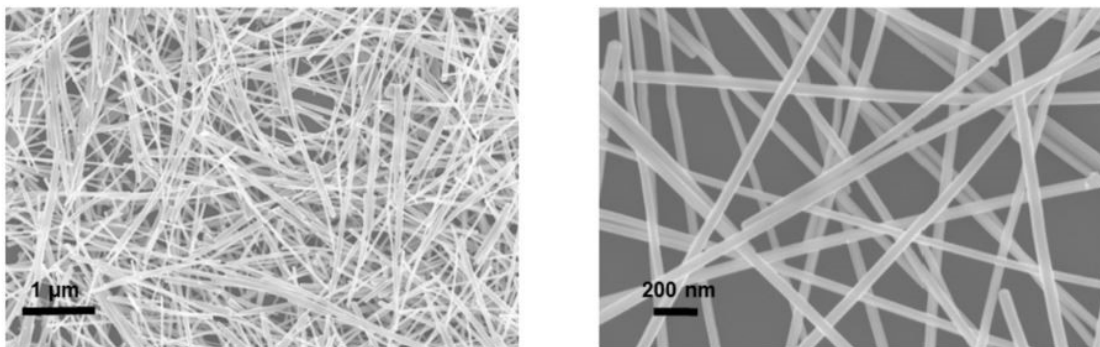


Figure 1.8 Scanning electron microscopy (SEM) images of silver nanowires at two magnifications. Reproduced with permission from Copyright Clearance Centre Marketplace for reference [58].

While AgNWs consist of metal, making this ink not the most environmentally friendly option, they do allow for fewer materials to be used compared to the alternative nanostructured inks.⁶² This advantage reduces the necessity for multiple printing passes and minimizes the particle loading within the ink formulation.^{54,61} Increasing the nanowire density contributes to enhancing the areal density and reducing sheet resistance, increasing the electrical conductivity of the resulting structures.⁵⁸ These features make AgNWs a promising choice for various printing techniques and applications, as they can be deposited with in fine lines and patterns. They are opted for in devices that require conductivity, material efficiency, and flexibility.

1.4 Paper-based Printed Electronic Devices

Using the knowledge of inks and substrates can aid in fine tuning which parameters to use when wanting to build devices. Devices that have been built using a paper substrate include: thermochromic and electrochromic displays, circuits, RFID tags, batteries, transistors, sensors, actuators.^{13,18,19,43,63,64} Many of these are multilayered devices in which multiple functional materials are deposited on the substrate to make the final product. Most applications require layers that are printable and buildable which allows for devices to become functional. With multiple layers the interface between layers will determine the functionality whereas subsequent layers have to wet and adhere to previous ones. Paper has shown that it is able to withstand the processes and has good device performance.

An area that is exciting is Light Emitting Diodes (LEDs) and their potential use in smart packaging. LEDs have been used in street illumination, display backlighting, and automotive lighting.⁶⁵ The field of light-emitting devices is attempting to follow suit and make the switch to using paper as the substrate to help mitigate the amount of e-waste.

Electroluminescence (EL), the process of emitting light due to the passage of an electric current through a material,⁶⁶ finds widespread use in displays and lighting applications.⁶⁷ These devices have been achieved in a few instances with Organic Light-Emitting Diodes (OLEDs) and Light-Emitting Electrochemical Cells (LEECs).⁶⁸⁻⁷⁰ Yoon and Moon (2012) made an OLED on copy paper with a parlyene and silicon oxide buffer layer on both sides of the substrate to cover the rough paper surface in order to fabricate the device.⁶⁹ The same ideology is followed by Asadpoordarvish et al (2015), where a barrier layer and a top coating or a planarizing layer were added to the paper for a LEEC to be created.⁶⁸ Since OLEDs require a planar substrate, Yao et al. (2016) integrated plastic into paper to create a plastic-paper substrate in which had benefits of both materials allowing for an OLED to be built on top.⁷⁰

Among light emitting devices is also Alternating Current Electroluminescence (ACEL) technology. With paper substrates, ACEL devices can be an interesting area to investigate for the creation of displaying information on packages. Within this area of chemistry, ACEL technology stands out with its unique advantages over other light-emitting devices like OLEDs and LEECs. While OLEDs and LEECs are also light-emitting technologies, ACELs offer distinct benefits such as the ability to be constructed on porous substrates and have more environmental stability.^{68,69,71}

1.41 Alternating Current Electroluminescence (ACEL) Devices

ACEL devices hold promise in fabrication of flexible, light-emitting devices. ACEL devices have been made on or with other flexible substrates, such as elastomers⁶⁶ or hydrogels⁷², plastics⁷³, and textiles⁷⁴, making it an ideal match with paper. Park et al. (2017) demonstrated the fabrication of a successful surface light-emitting transparent paper operated by AC voltages. Nanocellulose paper (NCP) in suspension was mixed with luminescent phosphors and then covered with AgNW to create the device.⁷⁵

The ACEL phosphors can also be easily combined with an elastomeric matrix, gaining intrinsic flexibility.^{66,67} As seen in Figure 1.9, Hu et al. (2019) created a flexible ACEL device using a polydimethylsiloxane (PDMS) fiber.⁶⁷ Specifically Figure 1.9c demonstrates that when the device is tied into a knot, they are still able to achieve light emission. The ability to integrate the phosphors into elastomers opens the possibilities for ACELs to become applicable in stretchable displays,^{66,72,76} conformable visual readouts in arbitrary shapes,^{67,76} and wearable electronic textiles.⁷⁴

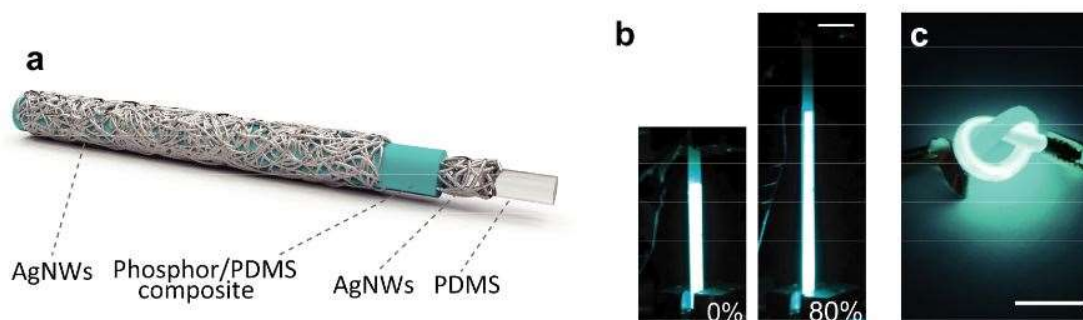


Figure 1.9 A stretchable ACEL fiber where a) shows the schematic of the device, b) Photographs show the original shape of the device (left) and when the fiber is subjected to a stretched strain of 80% (right), and c) Photograph of the knotted ACEL device. Adapted with permission from Creative Commons for reference [67].

ACELs work by using alternating current (AC) voltage to generate light. The basis of an ACEL device is the sandwiching of an emissive layer between two electrodes.⁷⁴ Figure 1.10 shows two different architectures of an ACEL.⁷⁷ This emissive material is composed of two parts: an organic or inorganic phosphor, often a phosphorescent or luminescent compound that determines the optoelectrical properties, and an insulator, the host material that dictates the electrical properties.

The mechanism of ACELs is explained by the impact ionization or impact excitation theories.⁶⁶ Pertaining to the impact ionization model, once subjected to a voltage, an AC electric field is generated, and electrons are propelled through the emissive material. The emissive material is composed of a phosphor lattice which upon collision with an electron creates electron-hole pairs. The recombination of these pairs is what is responsible for the luminescence.^{66,78} With the impact excitation model, the electrons

colliding with the localized luminescent centers of the emissive layer gives them energy, bringing the electron to an excited state. Upon the relaxation, energy is released in the form of a photon which gives off light.^{66,77} To facilitate the emission of light from the device, one of these electrodes must be transparent, allowing the produced light to escape.⁷⁷

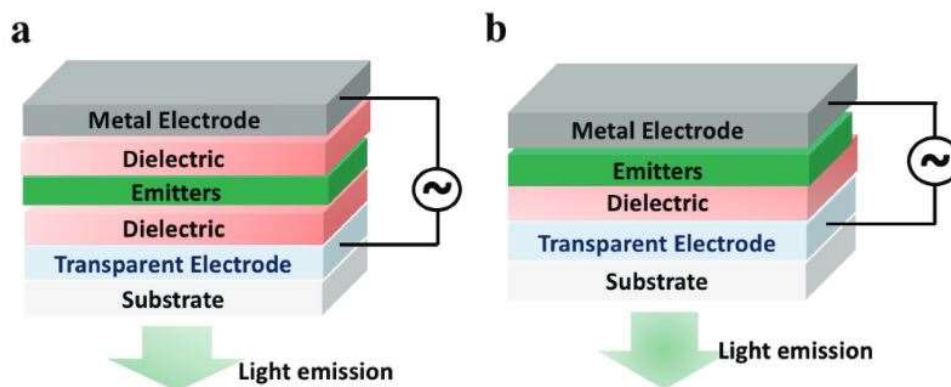


Figure 1.10 Schematics of ACELs with a) the symmetric and b) the asymmetric configurations, respectively. Reproduced with permission from Copyright Clearance Centre RightsLink for reference [77].

The color output of an ACEL device is mainly determined by the choice of phosphor material used. Most phosphors consist of compounds involving zinc, sulfide, or both elements. Within zinc sulfide phosphor particles, different dopants can be incorporated to emit varying wavelengths of light, resulting in a spectrum of colors.^{67,72} Dopants are elements that are introduced into the crystal lattice of compounds and change the electronic structure. The dopant that is very popular in these phosphors is copper, which will emit a blue colored light.⁶⁶ Other dopants, such as manganese or aluminum, will give off a different colored light due to the electronic composition being different.⁷⁹ In addition, altering the doping levels, adjusting the ultra-violet (UV) excitation wavelengths, or changing the frequency can tune the color and intensity.^{75,79} Adding multiple dopants, such as Park et al. (2006) did with manganese, copper, and chlorine, results in being able to get multiple colors by varying the ion concentrations and increasing the applied voltage.⁸⁰ This color-tuning capability adds to the versatility and visual appeal of ACEL displays and lighting solutions.

1.5 Scope of Thesis

This thesis aims to explore the relationship between paper substrates and functional inks for printed electronics. The research within this thesis works to bridge the gap in literature about how ink interacts with paper during printing. This knowledge can expand into creating a flexible multilayer device with light emitting capability using a paper substrate. Chapter 1 serves as an introduction to the materials used and to understand their characteristics individually. We outline the need for greener materials, how challenges within this field have been previously addressed, and the importance of making changes to improve device usage and performance in real-world applications.

In Chapter 2, we explore the relationship between pore size of paper and the properties of AgNW wicking into the paper. By investigating the wicking distance, the dynamics of drop spreading, and wicking dependence on nanomaterial dimensions we can draw conclusions on how certain parameters will impact printing resolution. We use various graded filter paper of defined pore size, different concentrations of AgNW solutions, and two different lengths of AgNWs to see trends in the wicking distance and speed, and electrical properties. We investigate trends of how AgNW solution interacts with the pores of paper that are either smaller or on the same scale as the lengths of the AgNWs. Even at small concentrations, AgNWs have great optical contrast, making it easy to analyze the wicking dynamics.

Then in Chapter 3, we use our ability to modify the porosity of papers using an alternative printing technique called DCP to fabricate a functional substrate for multilayered devices. Using this paper substrate, we can build up the layers of a device and create an ACEL that could be used in smart packaging. By studying each layer individually and at the interfaces we investigate the surface and electrical properties that allow for functionality of the device. This work can be continued by quantifying the light output from the paper-based ACEL device by taking optometer measurements. With the intention of using this ACEL in flexible applications, it would be of good interest to understand the performance after being subjected to bending experiments. With DCP printing showing promising results on this multilayer device more sophisticated patterns can be explored, or even looking to achieve patterns on different layers.

In Chapter 4, conclusions of this work and outlook on the field of printed electronics are discussed.

1.6 References

- (1) Bakar, K. B. A.; Zuhra, F. T.; Isyaku, B.; Sulaiman, S. B. A Review on the Immediate Advancement of the Internet of Things in Wireless Telecommunications. *IEEE Access* **2023**, *11*, 21020–21048. <https://doi.org/10.1109/ACCESS.2023.3250466>.
- (2) Coetzee, L.; Eksteen, J. The Internet of Things – Promise for the Future? An Introduction. **2011**.
- (3) Wortmann, F.; Flüchter, K. Internet of Things: Technology and Value Added. *Bus. Inf. Syst. Eng.* **2015**, *57* (3), 221–224. <https://doi.org/10.1007/s12599-015-0383-3>.
- (4) Khan, S.; Lorenzelli, L.; Dahiya, R. S. Technologies for Printing Sensors and Electronics Over Large Flexible Substrates: A Review. *IEEE Sens. J.* **2015**, *15* (6), 3164–3185. <https://doi.org/10.1109/JSEN.2014.2375203>.
- (5) Villamil, S.; Hernandez, C.; Tarazona, G. An Overview of Internet of Things. *TELKOMNIKA Telecommun. Comput. Electron. Control* **2020**, *18* (5), 2320. <https://doi.org/10.12928/telkomnika.v18i5.15911>.
- (6) Zheng, J.; Simplot-Ryl, D.; Bisdikian, C.; Mouftah, H. The Internet of Things [Guest Editorial]. *IEEE Commun. Mag.* **2011**, *49* (11), 30–31. <https://doi.org/10.1109/MCOM.2011.6069706>.
- (7) Realini, C. E.; Marcos, B. Active and Intelligent Packaging Systems for a Modern Society. *Meat Sci.* **2014**, *98* (3), 404–419. <https://doi.org/10.1016/j.meatsci.2014.06.031>.
- (8) Schaefer, D.; Cheung, W. M. Smart Packaging: Opportunities and Challenges. *Procedia CIRP* **2018**, *72*, 1022–1027. <https://doi.org/10.1016/j.procir.2018.03.240>.
- (9) Vanderroost, M.; Ragaert, P.; Devlieghere, F.; De Meulenaer, B. Intelligent Food Packaging: The next Generation. *Trends Food Sci. Technol.* **2014**, *39* (1), 47–62. <https://doi.org/10.1016/j.tifs.2014.06.009>.

- (10) Smits, E.; Schram, J.; Nagelkerke, M.; Kusters, R.; van Heck, G.; van Acht, V.; Koetse, M.; Centre, H. Development of Printed RFID Sensor Tags for Smart Food Packaging. **2012**.
- (11) Kang, H.; Park, H.; Park, Y.; Jung, M.; Kim, B. C.; Wallace, G.; Cho, G. Fully Roll-to-Roll Gravure Printable Wireless (13.56 MHz) Sensor-Signage Tags for Smart Packaging. *Sci. Rep.*
- (12) Kuswandi, B.; Wicaksono, Y.; Abdullah, A.; Heng, L. Y.; Ahmad, M. Smart Packaging: Sensors for Monitoring of Food Quality and Safety.
- (13) Puligundla, P. Carbon Dioxide Sensors for Intelligent Food Packaging Applications. *Food Control* **2012**.
- (14) Kate Bertrand Connolly. Johnnie Walker ‘Smart Bottle’ Performs for Consumers and Supply Chain Article-Johnnie Walker ‘Smart Bottle’ Performs for Consumers and Supply Chain. *Packaging Digest*. March 12, 2015.
<https://www.packagingdigest.com/beverage-packaging/johnnie-walker-smart-bottle-performs-consumers-and-supply-chain>.
- (15) Raghu Das and Dr Matthew Dyson. *Smart Packaging 2023-2033*; IDTechEx Research. <https://www.idtechex.com/en/research-report/smart-packaging-2023-2033/931>.
- (16) Neuvo, Y.; Ylönen, S. Bit Bang Rays to the Future. 286.
- (17) Hu, G.; Kang, J.; Ng, L. W. T.; Zhu, X.; Howe, R. C. T.; Jones, C. G.; Hersam, M. C.; Hasan, T. Functional Inks and Printing of Two-Dimensional Materials. *Chem. Soc. Rev.* **2018**, 47 (9), 3265–3300. <https://doi.org/10.1039/C8CS00084K>.
- (18) Tobjörk, D.; Österbacka, R. Paper Electronics. *Adv. Mater.* **2011**, 23 (17), 1935–1961. <https://doi.org/10.1002/adma.201004692>.
- (19) Jansson, E.; Lyytikäinen, J.; Tanninen, P.; Eiroma, K.; Leminen, V.; Immonen, K.; Hakola, L. Suitability of Paper-Based Substrates for Printed Electronics. *Materials* **2022**, 15 (3), 957. <https://doi.org/10.3390/ma15030957>.
- (20) Wu, W. Inorganic Nanomaterials for Printed Electronics: A Review. *Nanoscale* **2017**, 9 (22), 7342–7372. <https://doi.org/10.1039/C7NR01604B>.
- (21) Batet, D.; Vilaseca, F.; Ramon, E.; Esquivel, J. P.; Gabriel, G. Experimental Overview for Green Printed Electronics: Inks, Substrates, and Printing Techniques.

- Flex. Print. Electron.* **2023**, 8 (2), 024001. <https://doi.org/10.1088/2058-8585/acd8cc>.
- (22) Michael, S. S.; D'Amaral, G. M.; Carmichael, T. B. Debossed Contact Printing as a Patterning Method for Paper-Based Electronics.
- (23) Emamian, S.; Narakathu, B. B.; Chlaihawi, A. A.; Bazuin, B. J.; Atashbar, M. Z. Screen Printing for Flexible Piezoelectric Based Device on Polyethylene Terephthalate (PET) and Paper for Touch and Force Sensing Applications. *Sens. Actuators Phys.* **2017**, 263, 639-647. <https://doi.org/10.1016/j.sna.2017.07.045>.
- (24) Ali, A.; Williams, O.; Lester, E.; Greedy, S. High Code Density and Humidity Sensor Chipless RFID Tag. In *2022 7th International Conference on Smart and Sustainable Technologies (SpliTech)*; IEEE: Split / Bol, Croatia, 2022; pp 1–6. <https://doi.org/10.23919/SpliTech55088.2022.9854366>.
- (25) Chang, J. S.; Facchetti, A. F.; Reuss, R. A Circuits and Systems Perspective of Organic/Printed Electronics: Review, Challenges, and Contemporary and Emerging Design Approaches. *IEEE J. Emerg. Sel. Top. Circuits Syst.* **2017**, 7 (1), 7–26. <https://doi.org/10.1109/JETCAS.2017.2673863>.
- (26) Geyer, R.; Jambeck, J. R.; Law, K. L. Production, Use, and Fate of All Plastics Ever Made. *Sci. Adv.* **2017**, 3 (7), e1700782. <https://doi.org/10.1126/sciadv.1700782>.
- (27) Riechers, M.; Fanini, L.; Apicella, A.; Galván, C. B.; Blondel, E.; Espiña, B.; Kefer, S.; Keroullé, T.; Klun, K.; Pereira, T. R.; Ronchi, F.; Rodríguez, P. R.; Sardon, H.; Silva, A. V.; Stulgis, M.; Ibarra-González, N. Plastics in Our Ocean as Transdisciplinary Challenge. *Mar. Pollut. Bull.* **2021**, 164, 112051. <https://doi.org/10.1016/j.marpolbul.2021.112051>.
- (28) Habib, K.; Mohammadi, E.; Vihanga Withanage, S. A First Comprehensive Estimate of Electronic Waste in Canada. *J. Hazard. Mater.* **2023**, 448, 130865. <https://doi.org/10.1016/j.jhazmat.2023.130865>.
- (29) N. Perkins, D.; Brune Drisse, M.-N.; Nxele, T.; D. Sly, P. E-Waste: A Global Hazard. *Ann. Glob. Health* **2014**, 80 (4), 286. <https://doi.org/10.1016/j.aogh.2014.10.001>.

- (30) Hussein, R. N.; Schlingman, K.; Noade, C.; Carmichael, R. S.; Carmichael, T. B. Shellac-Paper Composite as a Green Substrate for Printed Electronics. *Flex. Print. Electron.* **2022**, *7* (4), 045007. <https://doi.org/10.1088/2058-8585/ac9f54>.
- (31) Nge, T. T.; Nogi, M.; Suganuma, K. Electrical Functionality of Inkjet-Printed Silver Nanoparticle Conductive Tracks on Nanostructured Paper Compared with Those on Plastic Substrates. *J. Mater. Chem. C* **2013**, *1* (34), 5235. <https://doi.org/10.1039/c3tc31220h>.
- (32) Institute of Home Economics, Delhi University, F-4, Hauz Khas Enclave, Near Hauz Khas Metro Station, New Delhi-110016, India; Jain, P.; Gupta, C. A Sustainable Journey of Handmade Paper from Past to Present: A Review. *Probl. Ekorozwoju* **2021**, *16* (2), 233–244. <https://doi.org/10.35784/pe.2021.2.25>.
- (33) Khan, S. M.; Nassar, J. M.; Hussain, M. M. Paper as a Substrate and an Active Material in Paper Electronics. *ACS Appl. Electron. Mater.* **2021**, *3* (1), 30–52. <https://doi.org/10.1021/acsaelm.0c00484>.
- (34) Adamopoulos, S.; Passialis, C. Grammage and Structural Density as Quality Indexes of Packaging Grade Paper Manufactured from Recycled Pulp. *Drew. Pr. Nauk. Doniesienia Komun.* **2014**, No. 191, 145–151. <https://doi.org/10.12841/wood.1644-3985.053.11>.
- (35) Ginebreda, A.; Guillén, D.; Barceló, D.; Darbra, R. M. Additives in the Paper Industry. In *Global Risk-Based Management of Chemical Additives I*; Bilitewski, B., Darbra, R. M., Barceló, D., Eds.; The Handbook of Environmental Chemistry; Springer Berlin Heidelberg: Berlin, Heidelberg, 2011; Vol. 18, pp 11–34. https://doi.org/10.1007/698_2011_109.
- (36) Hubbe, M. A.; Gill, R. A. Fillers for Papermaking: A Review of Their Properties, Usage Practices, and Their Mechanistic Role. *BioResources* **2016**, *11* (1), 2886–2963. <https://doi.org/10.15376/biores.11.1.2886-2963>.
- (37) Zhang, Y.; Zhang, L.; Cui, K.; Ge, S.; Cheng, X.; Yan, M.; Yu, J.; Liu, H. Flexible Electronics Based on Micro/Nanostructured Paper. *Adv. Mater.* **2018**, *30* (51), 1801588. <https://doi.org/10.1002/adma.201801588>.

- (38) Ahn, E.; Kim, T.; Jeon, Y.; Kim, B.-S. A4 Paper Chemistry: Synthesis of a Versatile and Chemically Modifiable Cellulose Membrane. *ACS Nano* **2020**, *14* (5), 6173–6180. <https://doi.org/10.1021/acsnano.0c02211>.
- (39) Cao, L.; Bai, X.; Lin, Z.; Zhang, P.; Deng, S.; Du, X.; Li, W. The Preparation of Ag Nanoparticle and Ink Used for Inkjet Printing of Paper Based Conductive Patterns. *Materials* **2017**, *10* (9), 1004. <https://doi.org/10.3390/ma10091004>.
- (40) Gaspar, C.; Sikanen, T.; Franssila, S.; Jokinen, V. Inkjet Printed Silver Electrodes on Macroporous Paper for a Paper-Based Isoelectric Focusing Device. *Biomicrofluidics* **2016**, *10* (6), 064120. <https://doi.org/10.1063/1.4973246>.
- (41) Shinde, D. H. Effect of Porosity of Paper on Printing in Different Printing Processes. **2018**, 3.
- (42) Kang, D. J.; González-García, L.; Kraus, T. Soft Electronics by Inkjet Printing Metal Inks on Porous Substrates. *Flex. Print. Electron.* **2022**, *7* (3), 033001. <https://doi.org/10.1088/2058-8585/ac8360>.
- (43) Guan, X.; Hou, Z.; Wu, K.; Zhao, H.; Liu, S.; Fei, T.; Zhang, T. Flexible Humidity Sensor Based on Modified Cellulose Paper. *Sens. Actuators B Chem.* **2021**, *339*, 129879. <https://doi.org/10.1016/j.snb.2021.129879>.
- (44) Zea, M.; Moya, A.; Villa, R.; Gabriel, G. Reliable Paper Surface Treatments for the Development of Inkjet-Printed Electrochemical Sensors. *Adv. Mater. Interfaces* **2022**, *9* (21), 2200371. <https://doi.org/10.1002/admi.202200371>.
- (45) Gozutok, Z.; Kinj, O.; Torun, I.; Ozdemir, A. T.; Onses, M. S. One-Step Deposition of Hydrophobic Coatings on Paper for Printed-Electronics Applications. *Cellulose* **2019**, *26* (5), 3503–3512. <https://doi.org/10.1007/s10570-019-02326-y>.
- (46) Tian, D.; Song, Y.; Jiang, L. Patterning of Controllable Surface Wettability for Printing Techniques. *Chem. Soc. Rev.* **2013**, *42* (12), 5184. <https://doi.org/10.1039/c3cs35501b>.
- (47) Glenn, G.; Shogren, R.; Jin, X.; Orts, W.; Hart-Cooper, W.; Olson, L. Per- and Polyfluoroalkyl Substances and Their Alternatives in Paper Food Packaging. *Compr. Rev. Food Sci. Food Saf.* **2021**, *20* (3), 2596–2625. <https://doi.org/10.1111/1541-4337.12726>.

- (48) Nery, E. W.; Kubota, L. T. Sensing Approaches on Paper-Based Devices: A Review. *Anal. Bioanal. Chem.* **2013**, *405* (24), 7573–7595. <https://doi.org/10.1007/s00216-013-6911-4>.
- (49) Lin, Y.; Gritsenko, D.; Liu, Q.; Lu, X.; Xu, J. Recent Advancements in Functionalized Paper-Based Electronics. *ACS Appl. Mater. Interfaces* **2016**, *8* (32), 20501–20515. <https://doi.org/10.1021/acsami.6b04854>.
- (50) Kamyshny, A. Metal-Based Inkjet Inks for Printed Electronics. *Open Appl. Phys. J.* **2011**, *4* (1), 19–36. <https://doi.org/10.2174/1874183501104010019>.
- (51) Nir, M. M.; Zamir, D.; Haymov, I.; Ben-Asher, L.; Cohen, O.; Faulkner, B.; De La Vega, F. Electrically Conductive Inks for Inkjet Printing. In *The Chemistry of Inkjet Inks*; WORLD SCIENTIFIC, 2009; pp 225–254. https://doi.org/10.1142/9789812818225_0012.
- (52) Cano-Raya, C.; Denchev, Z. Z.; Cruz, S. F.; Viana, J. C. Chemistry of Solid Metal-Based Inks and Pastes for Printed Electronics – A Review. *Appl. Mater. Today* **2019**, *15*, 416–430. <https://doi.org/10.1016/j.apmt.2019.02.012>.
- (53) Pekarovicova, A.; Husovska, V. Printing Ink Formulations. In *Printing on Polymers*; Elsevier, 2016; pp 41–55. <https://doi.org/10.1016/B978-0-323-37468-2.00003-8>.
- (54) Perelaer, J.; Smith, P. J.; Mager, D.; Soltman, D.; Volkman, S. K.; Subramanian, V.; Korvink, J. G.; Schubert, U. S. Printed Electronics: The Challenges Involved in Printing Devices, Interconnects, and Contacts Based on Inorganic Materials. *J. Mater. Chem.* **2010**, *20* (39), 8446. <https://doi.org/10.1039/c0jm00264j>.
- (55) Nayak, L.; Mohanty, S.; Nayak, S. K.; Ramadoss, A. A Review on Inkjet Printing of Nanoparticle Inks for Flexible Electronics. *J. Mater. Chem. C* **2019**, *7* (29), 8771–8795. <https://doi.org/10.1039/C9TC01630A>.
- (56) R., V. K. R.; K., V. A.; P. S., K.; Singh, S. P. Conductive Silver Inks and Their Applications in Printed and Flexible Electronics. *RSC Adv.* **2015**, *5* (95), 77760–77790. <https://doi.org/10.1039/C5RA12013F>.
- (57) Camargo, J. R.; Fernandes-Junior, W. S.; Azzi, D. C.; Rocha, R. G.; Faria, L. V.; Richter, E. M.; Muñoz, R. A. A.; Janegitz, B. C. Development of New Simple

- Compositions of Silver Inks for the Preparation of Pseudo-Reference Electrodes. *Biosensors* **2022**, *12* (9), 761. <https://doi.org/10.3390/bios12090761>.
- (58) Langley, D.; Giusti, G.; Mayousse, C.; Celle, C.; Bellet, D.; Simonato, J.-P. Flexible Transparent Conductive Materials Based on Silver Nanowire Networks: A Review. *Nanotechnology* **2013**, *24* (45), 452001. <https://doi.org/10.1088/0957-4484/24/45/452001>.
- (59) Li, Y.; Guo, S.; Yang, H.; Chao, Y.; Jiang, S.; Wang, C. One-Step Synthesis of Ultra-Long Silver Nanowires of over 100 Mm and Their Application in Flexible Transparent Conductive Films. *RSC Adv.* **2018**, *8* (15), 8057–8063. <https://doi.org/10.1039/C7RA13683H>.
- (60) Guan, P.; Zhu, R.; Zhu, Y.; Chen, F.; Wan, T.; Xu, Z.; Joshi, R.; Han, Z.; Hu, L.; Wu, T.; Lu, Y.; Chu, D. Performance Degradation and Mitigation Strategies of Silver Nanowire Networks: A Review. *Crit. Rev. Solid State Mater. Sci.* **2022**, *47* (3), 435–459. <https://doi.org/10.1080/10408436.2021.1941753>.
- (61) Patil, P.; Patil, S.; Kate, P.; Kulkarni, A. A. Inkjet Printing of Silver Nanowires on Flexible Surfaces and Methodologies to Improve the Conductivity and Stability of the Printed Patterns. *Nanoscale Adv.* **2021**, *3* (1), 240–248. <https://doi.org/10.1039/D0NA00684J>.
- (62) G. Nair, K.; Jayaseelan, D.; Biji, P. Direct-Writing of Circuit Interconnects on Cellulose Paper Using Ultra-Long, Silver Nanowires Based Conducting Ink. *RSC Adv.* **2015**, *5* (93), 76092–76100. <https://doi.org/10.1039/C5RA10837C>.
- (63) Zhang, Y.; Zuo, P.; Ye, B.-C. A Low-Cost and Simple Paper-Based Microfluidic Device for Simultaneous Multiplex Determination of Different Types of Chemical Contaminants in Food. *Biosens. Bioelectron.* **2015**, *68*, 14–19. <https://doi.org/10.1016/j.bios.2014.12.042>.
- (64) Liao, X.; Zhang, Z.; Liao, Q.; Liang, Q.; Ou, Y.; Xu, M.; Li, M.; Zhang, G.; Zhang, Y. Flexible and Printable Paper-Based Strain Sensors for Wearable and Large-Area Green Electronics. *Nanoscale* **2016**, *8* (26), 13025–13032. <https://doi.org/10.1039/C6NR02172G>.

- (65) Nian, L.; Pei, X.; Zhao, Z.; Wang, X. Review of Optical Designs for Light-Emitting Diode Packaging. *IEEE Trans. Compon. Packag. Manuf. Technol.* **2019**, *9* (4), 642–648. <https://doi.org/10.1109/TCPMT.2019.2895729>.
- (66) Zhang, X.; Wang, F. Recent Advances in Flexible Alternating Current Electroluminescent Devices. *APL Mater.* **2021**, *9* (3), 030701. <https://doi.org/10.1063/5.0040109>.
- (67) Hu, D.; Xu, X.; Miao, J.; Gidron, O.; Meng, H. A Stretchable Alternating Current Electroluminescent Fiber. *Materials* **2018**, *11* (2), 184. <https://doi.org/10.3390/ma11020184>.
- (68) Asadpoordarvish, A.; Sandström, A.; Larsen, C.; Bollström, R.; Toivakka, M.; Österbacka, R.; Edman, L. Light-Emitting Paper. *Adv. Funct. Mater.* **2015**, *25* (21), 3238–3245. <https://doi.org/10.1002/adfm.201500528>.
- (69) Yoon, D.-Y.; Moon, D.-G. Bright Flexible Organic Light-Emitting Devices on Copy Paper Substrates. *Curr. Appl. Phys.* **2012**, *12*, e29–e32. <https://doi.org/10.1016/j.cap.2011.04.033>.
- (70) Yao, S.; Zhu, Y. Wearable Multifunctional Sensors Using Printed Stretchable Conductors Made of Silver Nanowires. *Nanoscale* **2014**, *6* (4), 2345. <https://doi.org/10.1039/c3nr05496a>.
- (71) Lee, S.-M.; Kwon, J. H.; Kwon, S.; Choi, K. C. A Review of Flexible OLEDs Toward Highly Durable Unusual Displays. *IEEE Trans. Electron Devices* **2017**, *64* (5), 1922–1931. <https://doi.org/10.1109/TED.2017.2647964>.
- (72) Larson, C.; Peele, B.; Li, S.; Robinson, S.; Totaro, M.; Beccai, L.; Mazzolai, B.; Shepherd, R. Highly Stretchable Electroluminescent Skin for Optical Signaling and Tactile Sensing. *Science* **2016**, *351* (6277), 1071–1074. <https://doi.org/10.1126/science.aac5082>.
- (73) Wang, Z.; Chen, Y.; Li, P.; Hao, X.; Liu, J.; Huang, R.; Li, Y. Flexible Graphene-Based Electroluminescent Devices. *ACS Nano* **2011**, *5* (9), 7149–7154. <https://doi.org/10.1021/nn2018649>.
- (74) Wu, Y.; Mechael, S. S.; Chen, Y.; Carmichael, T. B. Solution Deposition of Conformal Gold Coatings on Knitted Fabric for E-Textiles and Electroluminescent

- Clothing. *Adv. Mater. Technol.* **2018**, 3 (3), 1700292.
<https://doi.org/10.1002/admt.201700292>.
- (75) Park, N.-M.; Koo, J. B.; Oh, J.-Y.; Kim, H. J.; Park, C. W.; Ahn, S.-D.; Jung, S. W. Electroluminescent Nanocellulose Paper. *Mater. Lett.* **2017**, 196, 12–15.
<https://doi.org/10.1016/j.matlet.2017.03.003>.
- (76) Wang, J.; Yan, C.; Cai, G.; Cui, M.; Lee-Sie Eh, A.; See Lee, P. Extremely Stretchable Electroluminescent Devices with Ionic Conductors. *Adv. Mater.* **2016**, 28 (22), 4490–4496. <https://doi.org/10.1002/adma.201504187>.
- (77) Wang, L.; Xiao, L.; Gu, H.; Sun, H. Advances in Alternating Current Electroluminescent Devices. *Adv. Opt. Mater.* **2019**, 7 (7), 1801154.
<https://doi.org/10.1002/adom.201801154>.
- (78) Bringuier, E. Electron Multiplication in ZnS-Type Electroluminescent Devices. *J. Appl. Phys.* **1990**, 67 (11), 7040-7044. <https://doi.org/10.1063/1.345051>.
- (79) Deng, Z.; Tong, L.; Flores, M.; Lin, S.; Cheng, J.-X.; Yan, H.; Liu, Y. High-Quality Manganese-Doped Zinc Sulfide Quantum Rods with Tunable Dual-Color and Multiphoton Emissions. *J. Am. Chem. Soc.* **2011**, 133 (14), 5389–5396.
<https://doi.org/10.1021/ja110996c>.
- (80) Park, J. H.; Lee, S. H.; Kim, J. S.; Kwon, A. K.; Park, H. L.; Han, S. D. White-Electroluminescent Device with ZnS:Mn, Cu, Cl Phosphor. *J. Lumin.* **2007**, 126 (2), 566–570. <https://doi.org/10.1016/j.jlumin.2006.10.012>.

CHAPTER 2
SYNCHRONIZING THE PORE SIZE OF PAPER SUBSTRATES AND ASPECT
RATIO OF SILVER NANOWIRES TO IMPROVE PRINTED ELECTRONICS

2.1 Introduction

The Internet of Things (IoT) era is driving the proliferation of electronic devices that are portable, flexible, lightweight, and even disposable. Device fabrication by printing solution-based functional inks is both economical and scalable, making this approach the preferred path forward for IoT devices such as sensors, batteries, and energy harvesters. Paper has been widely investigated as the substrate because it fulfills many of the requirements for ubiquitous IoT devices. Compared to commonly used plastic substrates such as poly(ethylene terephthalate) (PET), paper is a low-cost, sustainable, and biodegradable material. Paper is also compatible with scalable manufacturing methods such as roll-to-roll printing. The advantage that plastics have over paper, however, is that functional materials deposited on the surface form a distinct layer, contributing to good film quality, functional properties, and printing resolution.¹⁻³ In contrast, entangled cellulosic fibers give paper a porous structure, which promotes ink wicking. Dispersion of the functional ink within the paper pores can diminish the electrical performance of the printed material as well as compromise the printing resolution.⁴ However, the porosity of the substrate is not necessarily bad. Porous substrates provide new advantages, such as improving the adhesion of functional films through mechanical interlock, leading to mechanically robust devices⁵. Porous substrates have been reported to enhance the carrier transport efficiency in energy storage materials³ and reduce the stress concentration in active materials to prevent crack formation and device failure.⁶ To take advantage of these benefits in printed electronics (PE), it is essential to control the wicking of the functional ink into the porous substrate. This challenge can be addressed by optimizing the surface properties of the porous substrate, changing the composition and concentration of the functional ink, or modifying the printing parameters.⁵ Here, we explore a different approach to manage the wicking of 1D nanomaterial inks on paper substrates by investigating the relationship between the pore size of paper substrates and the length of silver nanowires (AgNWs). We show that the size ratio influences the wicking and dispersion of the AgNWs and can be optimized for the efficient use of the AgNW ink.

Chapter 2: Synchronizing the pore size of paper substrates and aspect ratio of silver nanowires to improve printed electronics

1D nanostructured materials such AgNWs have been widely used as conductors to fabricate electronic devices on both planar and porous substrates. AgNWs can be suspended in solution and then deposited using a variety of printing methods including inkjet,^{7,8} gravure,^{9,10} direct-writing,^{11,12} screen printing,¹³ and dip-coating.^{14,15} The deposited AgNWs form a network consisting of overlapping nanowires with AgNW-AgNW junctions.^{16,17} Sintering fuses the AgNW-AgNW junctions together, reducing the contact resistances within the network to provide high electrical conductivity.^{16,18} The optical transparency provided by the openings between AgNWs in the network makes AgNWs extremely well-studied as transparent conducting electrodes for optoelectronics. An important advantage of AgNWs over other silver-based inks is the mechanical flexibility of the network, making them ideal for flexible and even stretchable electronics.^{13,19} Because of these benefits, AgNWs have been used as conductive elements in flexible paper-based electronics. For example, combining AgNWs with paper by dip-coating, spray-coating, or filtration produces mechanically flexible AgNW-paper composites that are highly effective at electromagnetic interference (EMI) shielding. Replacing the conventional paper substrate with an optically transparent cellulose nanopaper provides cellulose/AgNW transparent conducting electrodes.²⁰

When it comes to patterning AgNWs on paper to create paper-based circuits, researchers have investigated several different approaches to control the wicking of AgNW-based inks. The most common approach is to coat the paper surface with a polymer or wax layer to fill in the pores, creating a planar surface that prevents the diffusion and penetration of the ink.²¹⁻²³ Examples of this approach include inkjet printing or direct writing of AgNW inks on photo paper or inkjet paper. However, this approach eliminates the benefits of the porosity, introduces polymeric layers into the system that add cost and weight, and may compromise the recyclability of the paper.²³ A study of AgNW inks printed by direct writing onto coated and uncoated paper substrates highlight the advantages and disadvantages of the nature of the paper substrate. While capacitive touch sensors fabricated on uncoated paper showed better durability to repeated mechanical deformation, the AgNWs also diffused to about 5 μm and

consequently showed lower conductance properties compared to AgNWs on coated paper.¹¹ Methods to retain the porosity of the paper substrate while controlling wicking of the AgNW ink include the printing-filtration-press (PFP) technique, in which the paper substrate is pre-patterned with a pore-filling material, and then AgNWs are deposited in the unpatterned regions by vacuum filtration. A similar method pre-patterns the paper substrate with polyimide tape and then deposits AgNWs via drop casting. Another approach avoids wicking altogether by patterning the AgNWs on a carrier substrate and then transferring the patterned network to the paper substrate.^{13,19,24}

Here, we show that the pore size of the paper substrate and the length of the AgNWs are useful parameters to optimize the electrical performance of AgNW inks deposited on paper. These parameters affect the wicking and dispersion of the ink, either restricting the AgNWs at the surface of the paper or enabling the AgNWs to wick downwards into the paper. Optimizing these parameters together is potentially a new aspect of the device design of printed electronics based on 1D nanomaterial inks.

2.2 Results and Discussion

We studied the deposition and wicking of AgNWs suspended in ethanol on Whatman cellulose filter paper. We chose filter paper as the substrate for two reasons: First, filter paper is a widely available, inexpensive commodity commonly used in laboratories. Second, filter paper is commercially available with different pore sizes. The pore size provided by the manufacturer corresponds to the largest sphere that can pass through the filter paper. We used filter papers with nominal pore sizes of 2.5, 8, 11, and 20-25 μm .

Chapter 2: Synchronizing the pore size of paper substrates and aspect ratio of silver nanowires to improve printed electronics

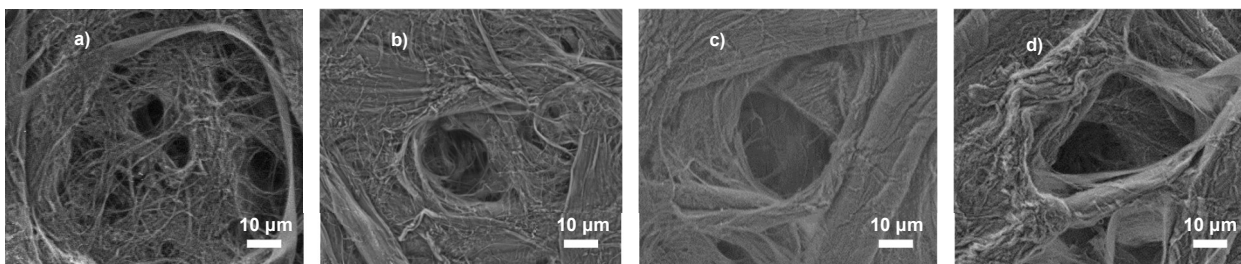


Figure 2.1 SEM characterization at 1500x magnification of filter paper of pore sizes a) 2.5 μm b) 8 μm c) 11 μm and d) 20-25 μm .

Scanning electron micrographs (SEM) show the variation in pore size of the filter papers (**Figure 2.1**). Silver nanowires (AgNWs) are commercially available in various dimensions that range in length and diameter.^{18,25} We used AgNWs with a width of 90-100 nm and two different lengths: AgNW30s, which have a length of 20-30 μm , and AgNW200s, which have a length of 100-200 μm . We used suspensions of AgNW30s and AgNW200s in concentrations of 0.4, 0.7, 2, and 3 mg/mL in ethanol, and deposited 10 μL onto 1 cm^2 pieces of filter paper. We used an optical microscope to record videos of the wicking and drying of the deposited AgNW solutions and measured the diameter of the visible AgNW network at time intervals as the solvent evaporated. To characterize the composite electrically 60 $\mu\text{L}/\text{cm}^2$ of AgNW suspensions were deposited onto the 1 cm^2 pieces of filter paper and allowed to dry. After evaporation, we annealed the samples at 190 $^\circ\text{C}$ for 30 minutes on a hot plate to remove residual solvent and fuse the AgNWs at their junction points to form a robust and conductive network.¹⁸

Chapter 2: Synchronizing the pore size of paper substrates
and aspect ratio of silver nanowires to improve printed electronics

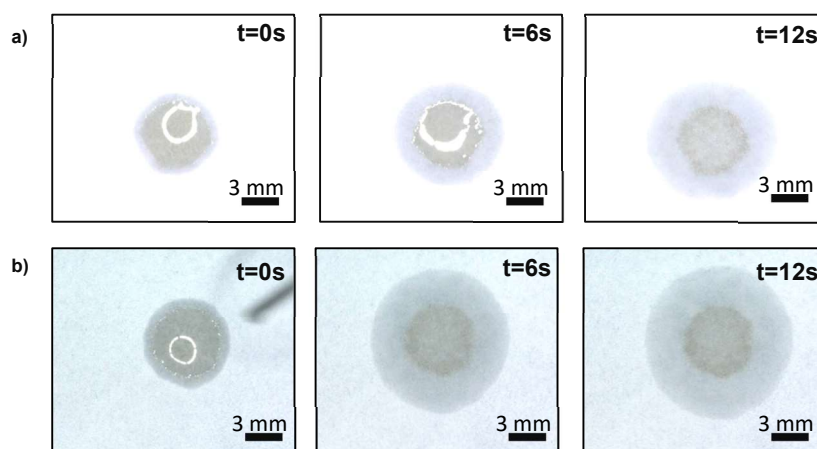


Figure 2.2 Still images of 10 µL of 3 mg/mL AgNW30 solution in ethanol at zero, six and twelve seconds after deposition on filter paper of pore size a) 2.5 µm and b) 20-25 µm.

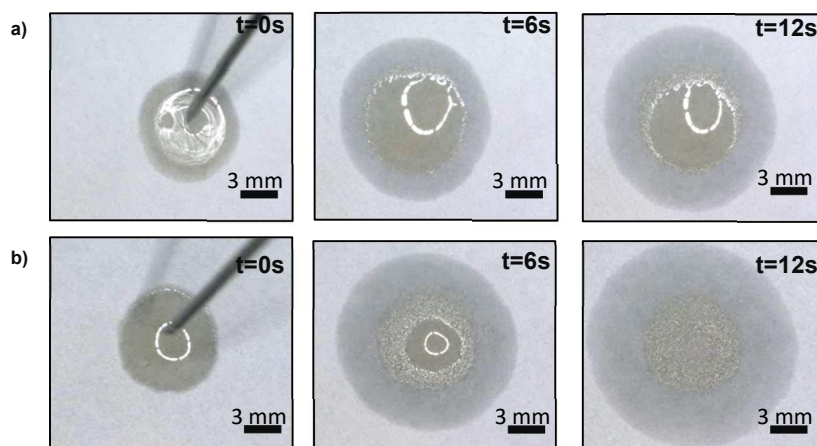


Figure 2.3 Still images of 10 µL of 3 mg/mL AgNW200 solution in ethanol at zero, six, and twelve seconds on filter paper of pore size a) 2.5 µm and b) 20-25 µm.

Figures 2.2 and **2.3** compare still images at different time intervals after drop casting AgNW30 and AgNW200 suspensions (3 mg/mL) on filter papers of the smallest and largest pore sizes. The images show the spreading and evaporating solvent front surrounding the area of deposition of the AgNW networks. As the ethanol solvent wicks through the filter paper, it carries and deposits AgNWs.

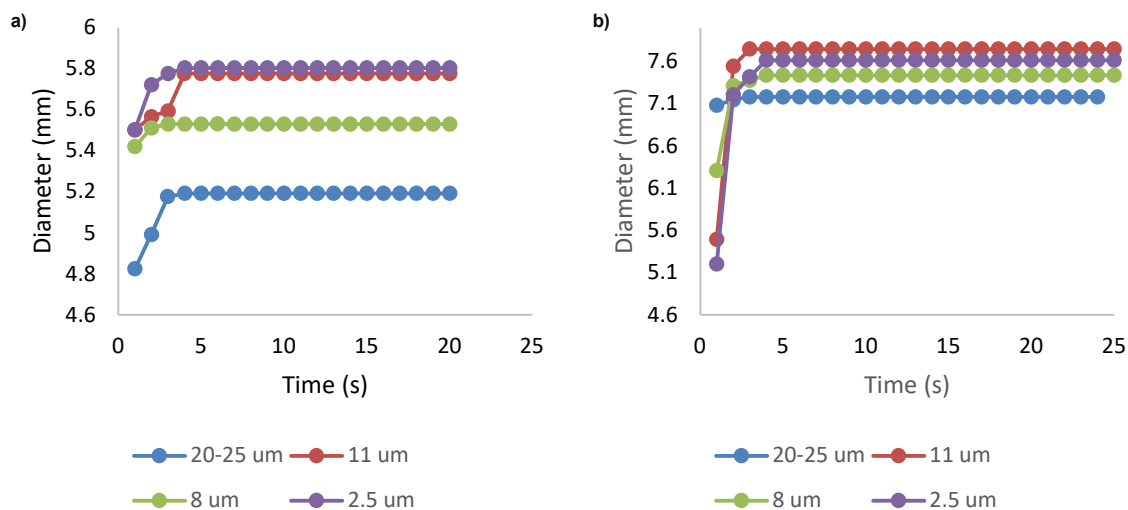


Figure 2.4 Maximum lateral wicking diameter over time for the AgNW front for a) AgNW30 b) AgNW200. Data was collected from video stills and correspond to a single sample.

We measured the diameter of the AgNW network over time to quantify the extent of the dispersion (**Figure 2.4, Table S2.1**). The lateral dispersion of both AgNW30 and AgNW200 solutions depends on both the pore size of the filter paper and the length of the AgNWs. In general, as the pore size of the filter paper increases, the diameter of the AgNW network decreases for both AgNW30 and AgNW200 suspensions. Figures 2.2 and 2.3 show that pooling of the AgNW solutions on filter paper of small (2.5 μm) pore size persists for a longer time compared to drops deposited on filter paper of larger (20-25 μm) pore sizes. These observations suggest that small pore sizes limit wicking of the suspension of AgNWs downwards into the paper, leading to lateral spreading of the drop, whereas larger pore sizes permit wicking of the AgNW suspensions downwards into the paper and result in less lateral spreading. A comparison of the diameters of AgNW30 and AgNW200 networks shows that the length of the AgNWs has a substantial effect on the wicking of the suspensions. The diameters of AgNW200 networks on all filter papers are larger than those of AgNW30 network, suggesting that the longer AgNWs impede wicking downwards into the paper and result in more lateral spreading.

Chapter 2: Synchronizing the pore size of paper substrates
and aspect ratio of silver nanowires to improve printed electronics

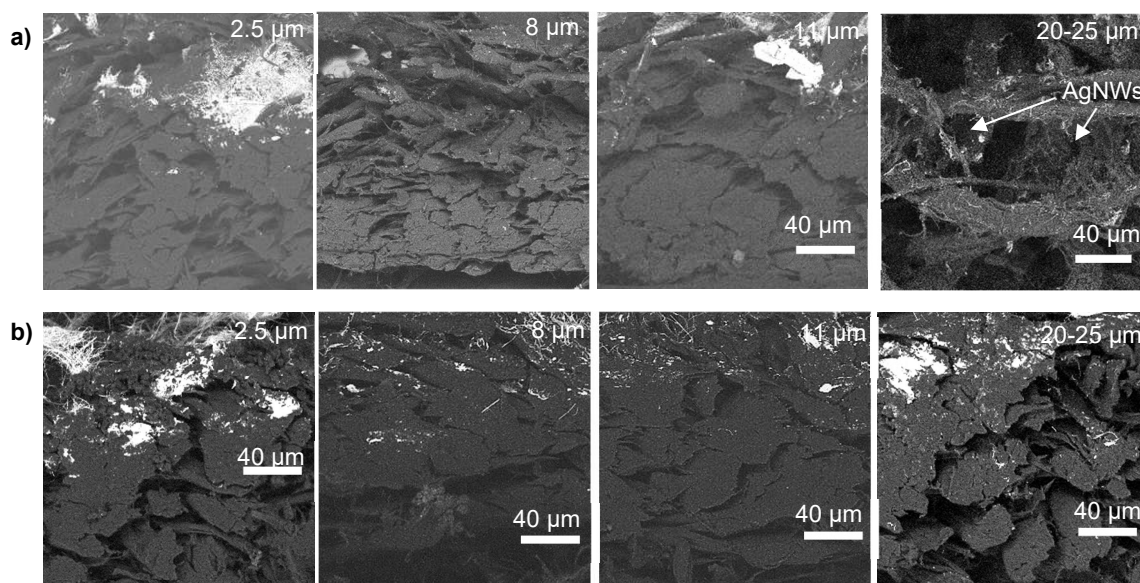


Figure 2.5 Cross-sectional SEM of 3 mg/mL AgNW solutions deposited on filter paper of at 2.5 μm , 8 μm , 11 μm and, 20-25 μm at 600x magnification a) AgNW30 b) AgNW200.

We probed the wicking of the AgNW suspensions into the paper by scanning electron microscopy (SEM). Silver provides high elemental contrast in these images, with the AgNWs appearing brighter than the paper. Although cross-sectional SEM images are an ideal way to determine the wicking depth, in practice it was difficult to obtain a clean edge when cleaving the paper substrates. Nonetheless, images of 3 mg/mL dispersions deposited on filter paper qualitatively show that, in general, the AgNWs penetrate further into the paper with large pores compared to small pores (**Figure 2.5**). In addition, the AgNW30s penetrate deeper into the filter paper with the largest pore size (20-25 μm) compared to the AgNW200s.

Chapter 2: Synchronizing the pore size of paper substrates
and aspect ratio of silver nanowires to improve printed electronics

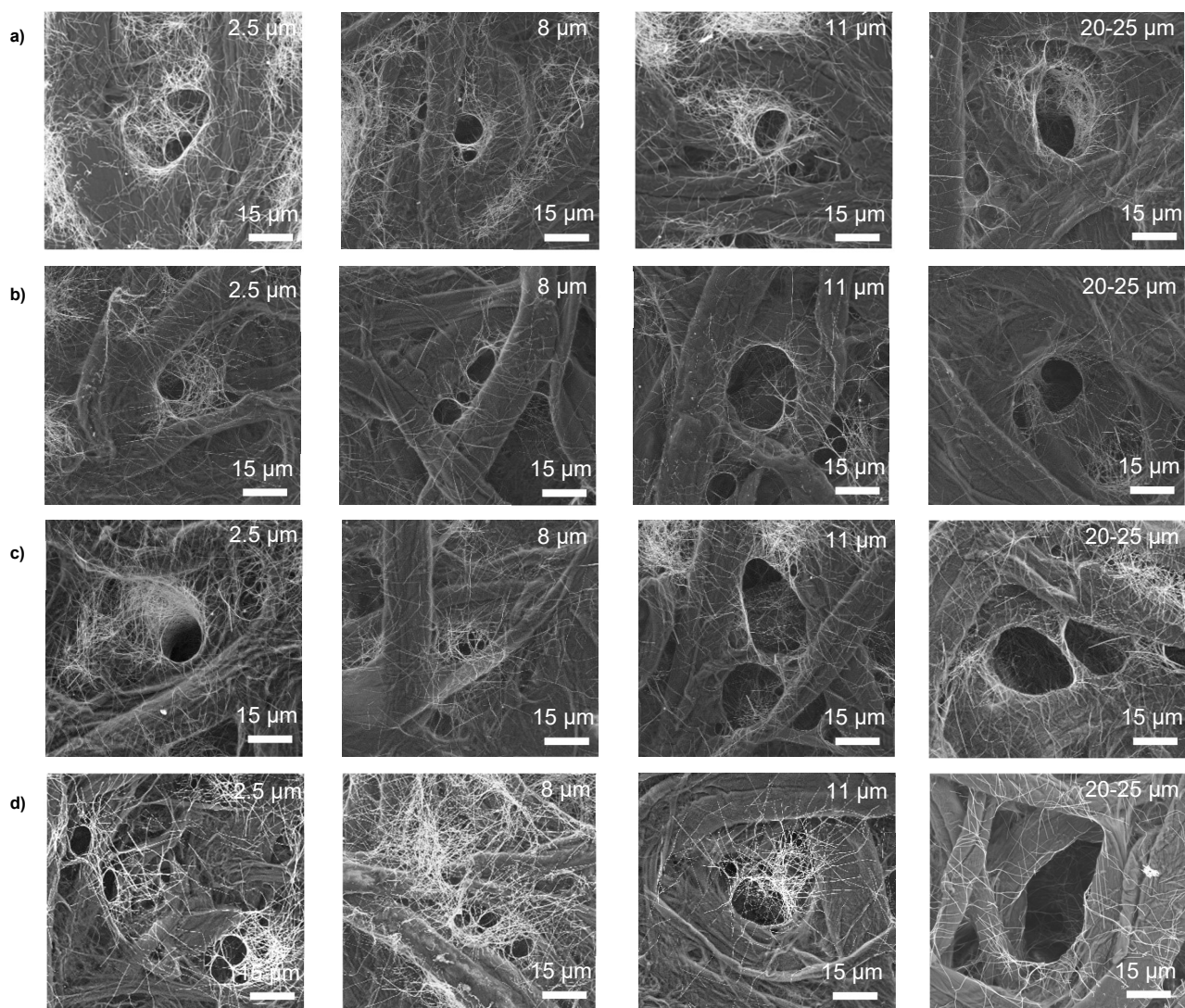


Figure 2.6 SEM characterization at 1500x magnification of AgNW30 solution on filter paper with pore sizes of 2.5 μm, 8 μm, 11 μm, and 20-25 μm at concentrations of a) 3 mg/mL b) 2 mg/mL c) 0.7 mg/mL and d) 0.4 mg/mL.

Top-down SEM images also show how the pore size and AgNW length affects the interaction of the AgNWs with the paper (**Figures 2.6 and 2.7**). The AgNW30s aggregate on the surface of filter papers with small pore sizes, which is particularly pronounced for the most concentrated (3 mg/mL) AgNW30 suspensions (**Figure 2.6a**). As the pore size increases, there is less aggregation at the surface. Instead, AgNW30s

Chapter 2: Synchronizing the pore size of paper substrates
and aspect ratio of silver nanowires to improve printed electronics

wrap around the paper fibers and line the inside of the pores. This penetration into the pores is evident for all concentrations of AgNW30 suspensions used for the deposition.

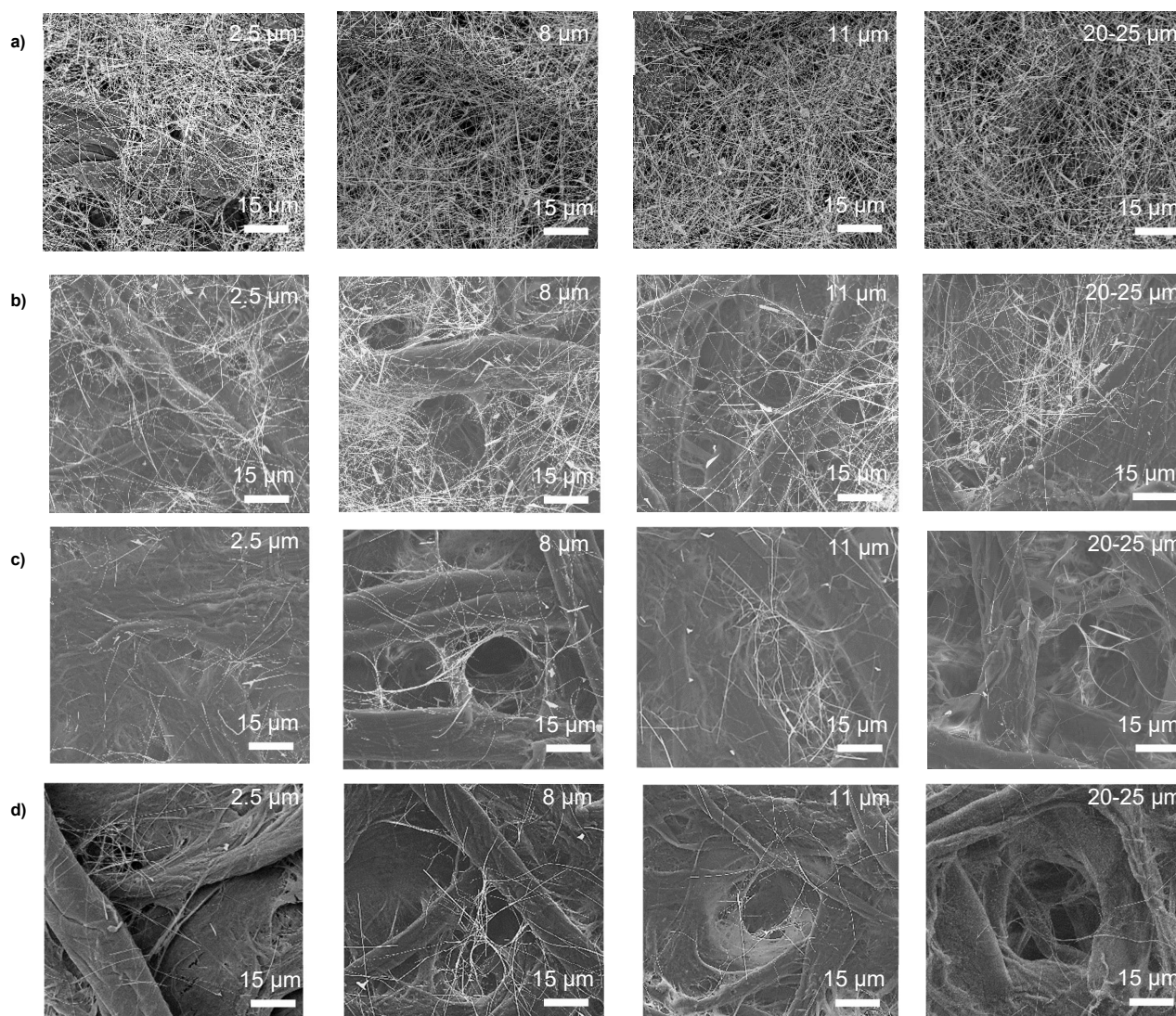


Figure 2.7 SEM characterization at 1500x magnification of AgNW200 solution on filter paper with pore sizes of 2.5 μm, 8 μm, 11 μm, and 20-25 μm at concentrations of a) 3 mg/mL b) 2 mg/mL c) 0.7 mg/mL and d) 0.4 mg/mL.

SEM images of the edge of the AgNW30 network support this interpretation, with a higher concentration of AgNW30s appearing at the surface of filter paper with the smallest pores. As the pore size increases, the AgNW30s wick into the surface of the filter paper, diminishing the contrast in the SEM (**Figure 2.8**). The AgNW200s also aggregate on the surface of the paper; however, the effect is more pronounced than for

Chapter 2: Synchronizing the pore size of paper substrates
and aspect ratio of silver nanowires to improve printed electronics

AgNW30 networks (**Figure 2.7**). At the highest concentration (3 mg/mL), the AgNW200s cover the pores of all sizes, forming a dense network on the surface. We postulate that entanglement of the AgNW200s may impede the movement of AgNW200s into the pores. As the concentration of the AgNW200 suspension decreases, the network becomes less dense, and the pore structure of the filter paper becomes visible. In contrast to the AgNW30s, SEM images of the edge of the AgNW200 network show contrast that is unchanged by the pore size, supporting the idea that AgNW200s are too long and entangled to substantially penetrate even the largest pores (**Figure 2.9**).

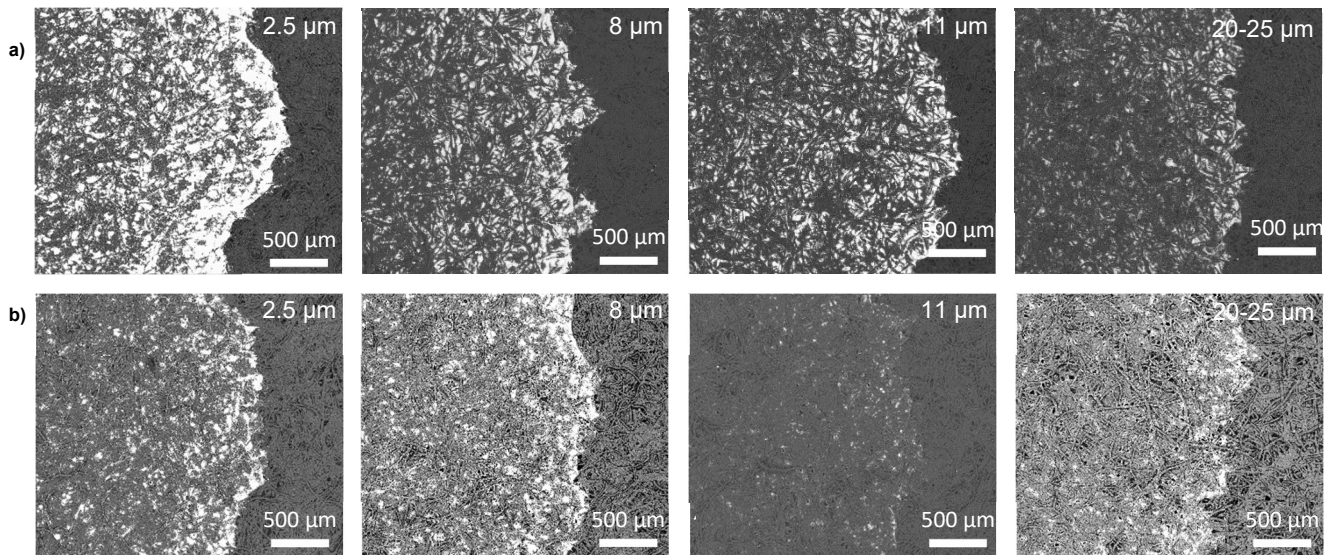


Figure 2.8 SEM characterization of the edge of the AgNW30 front on filter paper with pore size 2.5 μm, 8 μm, 11 μm, and 20-25 μm at concentrations of a) 0.4 mg/mL and b) 3 mg/mL.

Chapter 2: Synchronizing the pore size of paper substrates and aspect ratio of silver nanowires to improve printed electronics

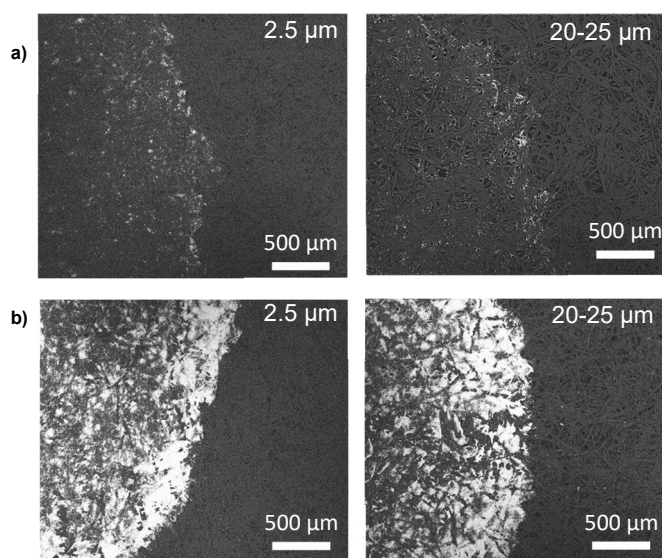


Figure 2.9 SEM characterization of the edge of the AgNW200 front on filter paper with pore size 2.5 μm and 20-25 μm at concentrations of a) 0.4 mg/mL and b) 3 mg/mL.

The ramifications of the length of the AgNWs and how they interact with filter paper of different pore sizes become evident in the conductivity of the networks. For both the AgNW30 and AgNW200 networks, increasing the concentration of the AgNW suspensions deposited on the paper substrate results in networks composed of more AgNWs and more AgNW-AgNW junctions; thus, as the concentration of the AgNWs increases, the sheet resistance decreases (**Figure 2.10**). This trend holds for both AgNW30 and AgNW200 networks and filter papers of each pore size. In addition, at each concentration, networks of the AgNW200 exhibit lower sheet resistances compared to networks the AgNW30. Langley et al. (2013) report that longer AgNWs due to their length do not need as many wires as shorter AgNWs do to achieve conductivity.¹⁸ This is a known effect and happens because their length offers more entanglement but a lower requirement for the number of AgNW-AgNW junctions are needed for the longer AgNWs since they are able to cover more area.^{18,26}

Chapter 2: Synchronizing the pore size of paper substrates
and aspect ratio of silver nanowires to improve printed electronics

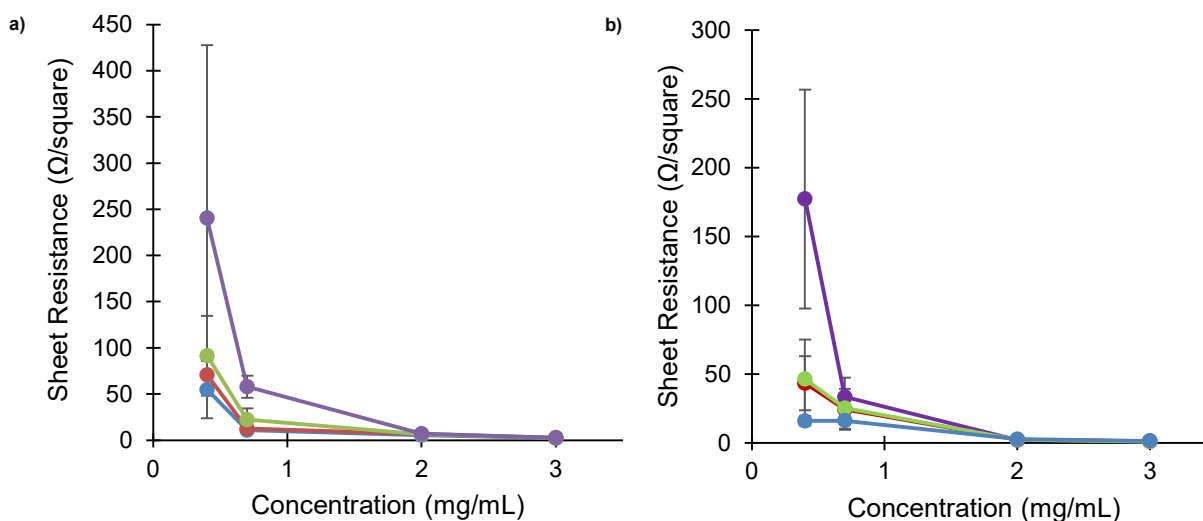


Figure 2.10 Sheet resistance of a) AgNW30 and b) AgNW200 in relation to concentration and pore sizes of 2.5 μm (blue), 8 μm (red), 11 μm (green), and 20-25 μm (purple). Bars correspond to standard deviation.

Table 2.1 Sheet resistance values in relation to concentration and pore size for a) AgNW30, b) AgNW200

a)		Pore Size (μm)			
		2.5	8	11	20-25
Concentration (mg/mL)	0.4	54.97 ± 31.01 Ω/sq	70.88 ± 16.71 Ω/sq	91.64 ± 43.12 Ω/sq	240.61 ± 187.52 Ω/sq
	0.7	10.82 ± 2.79 Ω/sq	12.60 ± 3.24 Ω/sq	22.35 ± 12.09 Ω/sq	57.95 ± 12.06 Ω/sq
	2	5.24 ± 5.24 Ω/sq	6.54 ± 2.48 Ω/sq	6.40 ± 2.53 Ω/sq	6.93 ± 2.55 Ω/sq
	3	2.26 ± 1.03 Ω/sq	2.51 ± 0.61 Ω/sq	2.59 ± 0.96 Ω/sq	2.76 ± 0.77 Ω/sq

b)		Pore Size (μm)			
		2.5	8	11	20-25
Concentration (mg/mL)	0.4	16.08 ± 31.01 Ω/sq	46.45 ± 19.66 Ω/sq	43.49 ± 28.86 Ω/sq	177.39 ± 79.53 Ω/sq
	0.7	16.21 ± 5.81 Ω/sq	25.41 ± 14.93 Ω/sq	24.48 ± 7.62 Ω/sq	33.54 ± 13.97 Ω/sq
	2	2.57 ± 0.62 Ω/sq	2.41 ± 0.79 Ω/sq	2.38 ± 0.65 Ω/sq	2.07 ± 0.28 Ω/sq
	3	1.54 ± 0.24 Ω/sq	1.12 ± 0.18 Ω/sq	1.25 ± 0.21 Ω/sq	1.34 ± 0.31 Ω/sq

For both AgNW30 and AgNW200 networks, the pore size of the filter paper does not influence the sheet resistance values for networks formed using AgNW concentrations > 2 mg/mL (Table 2.1). As the AgNW concentration decreases to 0.7 mg/mL and 0.4 mg/mL, however, the influence of the pore size on the sheet resistance values becomes apparent (Figure 2.11, Table 2.1). Figure 2.11 shows that the sheet resistance values of the sparse networks formed using both AgNW30 and AgNW200 increase as the pore size of the filter paper increases.

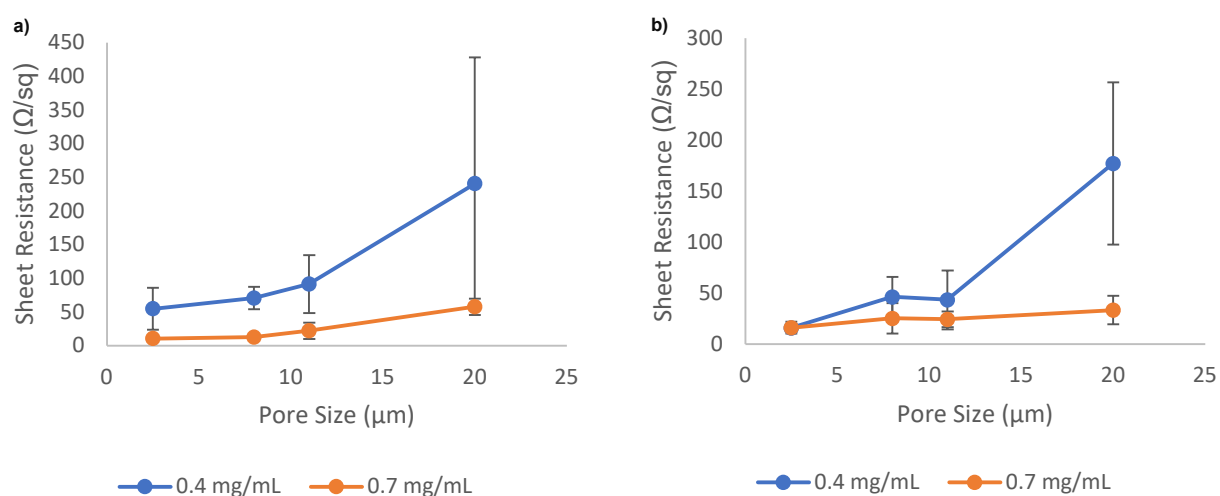


Figure 2.11 Sheet resistance in relation to pore sizes for 0.4 mg/mL solution (blue) and 0.7 mg/mL solution (orange) for a) AgNW30 and b) AgNW200. Bars correspond to standard deviation.

We postulate that larger pores enable wicking of the AgNWs downwards into the paper, to form a dispersed – but still conductive – network. In contrast, smaller pores keep the AgNWs at the surface to form a more compact network with more AgNW-AgNW junctions. This interpretation is consistent with the wicking diameters of Figures 2.2 and 2.3. Overall, we find that sheet resistance values can be dialed in through the choice of pore size, AgNW length, and AgNW concentration. For PE applications requiring low resistance, it is optimal to use concentrations of AgNWs > 2 mg/mL. At these concentrations, the dense AgNW networks dominate the electrical performance, and penetration of the AgNWs into even the largest pores does not measurably affect the electrical performance. For applications with less stringent conductivity requirements, it

is possible to economize the use of AgNWs by using lower concentrations. In this concentration regime, the pore size of the paper should be as small as possible to optimize the electrical performance of these sparse networks. For example, sheet resistances of $< 20 \Omega/\text{sq}$ are possible using AgNW concentrations as low as 0.4 mg/mL when the pore size of the paper is small ($2.5 \mu\text{m}$) and long AgNWs are selected. We note that there is room for improvement of the standard deviations of sheet resistance values at these lower concentrations. We attribute the variation to non-uniformity in the AgNW network structures, which may be improved by optimizing the ink formulation and wettability of the paper fibers.

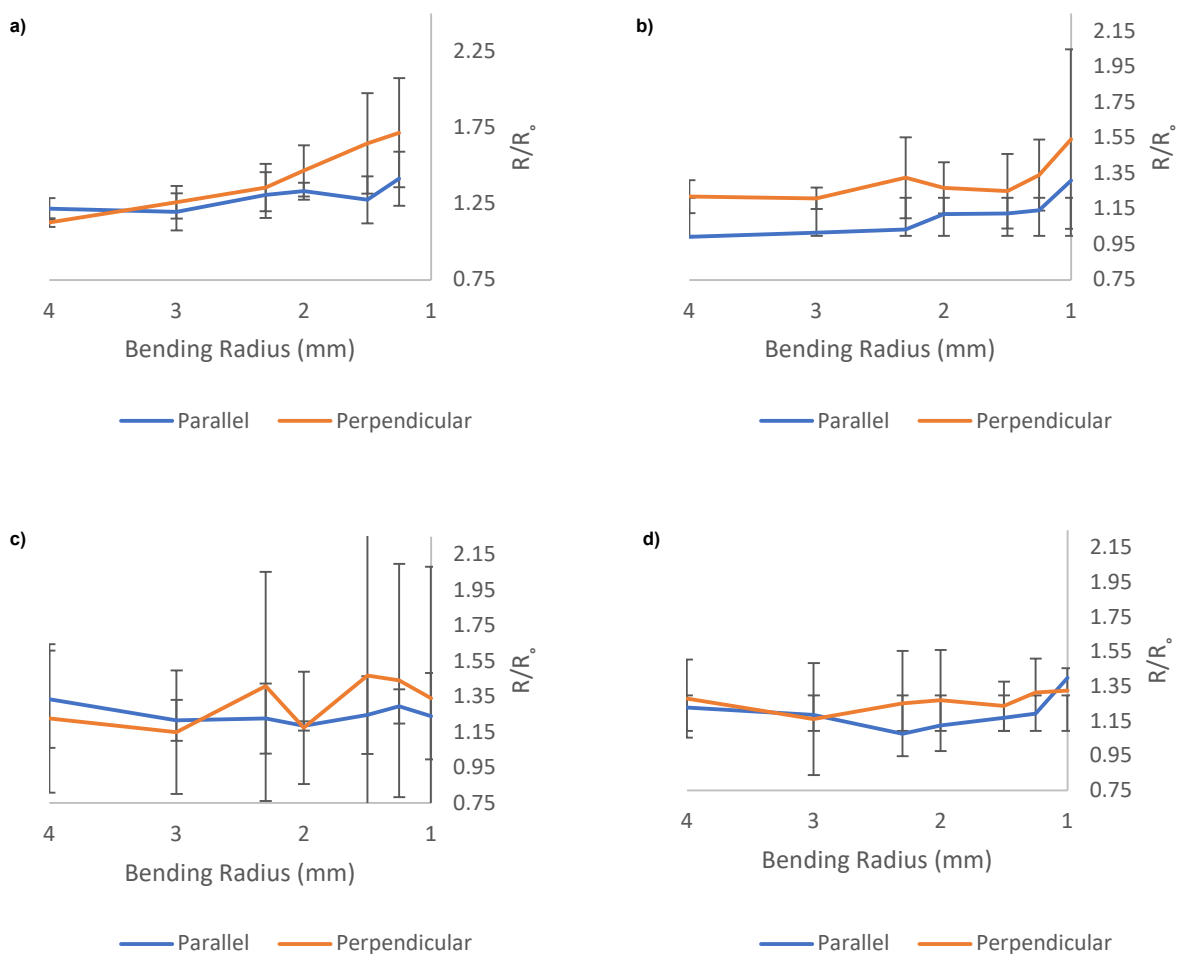


Figure 2.12 Change in resistance during bending of 3 mg/mL AgNW30 on filter paper of pore size a) 20-25 μm b) 11 μm c) 8 μm d) 2.5. Bars correspond to standard deviation.

Chapter 2: Synchronizing the pore size of paper substrates and aspect ratio of silver nanowires to improve printed electronics

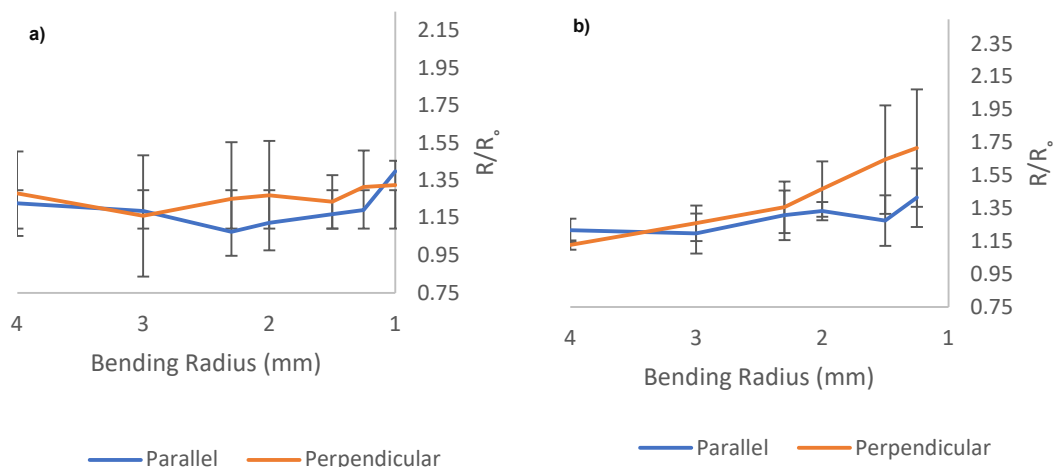


Figure 2.13 Change in resistance during bending of 3 mg/mL of a) AgNW30 and b) AgNW200 on filter paper of pore size 2.5 μm . Bars correspond to standard deviation.

Finally, we conducted preliminary testing of the mechanical properties of AgNW30s and AgNW200s (3 mg/mL) deposited on filter papers. Bending 1 cm² samples to radii from 4 mm to 1 mm resulted in no significant change in resistance values, regardless of AgNW length or the pore size of the paper (**Figures 2.12 and 2.13**). Further work to quantify the bendability of optimized sparse networks formed using low concentrations of AgNWs will add to the ability to design AgNW networks for specific applications in PE.

2.3 Conclusion

The work described here opens a new avenue for the design of PE devices using 1D nanomaterial inks. By careful selection of AgNW length and the pore size of the filter paper, it is possible to control the lateral spreading of the ink and minimize the concentration of the AgNWs to achieve a specific electrical performance. Future work will expand this study in two ways: First, it is important to extend this work to include paper substrates that can be used for mass production of PE, such as roll-to-roll printing. The findings presented here on filter paper can be used as guidelines to select printing

paper with the appropriate pore size to maximize electrical performance and control lateral wicking. Second, extending the study to other 1D nanomaterial inks, such as carbon nanotubes, will be an important step toward greener, metal-free PE.

2.4 Experimental

Materials: Stock AgNW solutions (20 mg/mL in ethanol) with nanowire diameters of 90-100 nm and lengths of 20-30 μm (AgNW30) and 100- 200 μm (AgNW200) were purchased from Advanced Chemicals Supplier (California). Whatman filter paper with pore sizes of 2.5 μm , 8 μm , 11 μm , and 20-25 μm was purchased from VWR (Pennsylvania).

Silver Nanowire Solution Preparation: The AgNW stock solutions were shaken by hand for approximately a minute. The required amount of AgNW stock solutions were deposited into a vial using a micropipette. The AgNW30 stock solution vials were then sonicated at 42 kHz using a Branson Ultrasonic Cleaner 1510R-MTH for 1 minute. The stock solution was then diluted with the required volume of anhydrous ethanol using a micropipette to 0.4 mg/mL, 0.7 mg/mL, 2 mg/mL, or 3 mg/mL solutions, respectively. They were then again shaken by hand and sonicated again for 1 minute. The AgNW200 stock solution was diluted with the required volume of anhydrous ethanol using a micropipette to 0.4 mg/mL, 0.7 mg/mL, 2 mg/mL, or 3 mg/mL solutions, respectively. They were then shaken by hand and partially sonicated using the same equipment with the same conditions but only for a duration of 35 seconds.

Deposition of AgNWs on Filter Paper Substrates: Filter paper with pore sizes of 2.5 μm , 8 μm , 11 μm , and 20-25 μm were cut to 1 cm^2 squares. The filter paper was suspended using a homemade holder to prevent any solvent from wicking off. The AgNW solution was deposited with a micropipette held directly perpendicular and centered over the filter paper. The amount deposited was either 10 μL for the video analysis or 60 $\mu\text{L}/\text{cm}^2$ for sheet resistance. The AgNW/paper composites were left suspended for 15 minutes to dry, and then annealed on a hot plate at 190°C for 30 minutes to fuse the AgNW-AgNW junctions.

Characterization: Optical micrographs of the drops and videos of the advancing solvent and nanowire front were collected using a Keyence Digital Microscope VHX-6000 Series. Drop diameters were measured using the program Q Capture Pro 6.0. Data extraction stills were collected from the video in 1 second increments. Drop diameter measurements are an average of at least six samples. Scanning electron microscope (SEM) images were collected using a Quanta 200 FEG Environmental Scanning Electron Microscope (SEM) using 20 kV, a spot size of 3, and a working distance of ~10 mm. Sheet resistances were measured using a Keithley 2601 System Source Meter, using a 4-point probe setup. Measurements were taken in all four directions and averaged. Reported sheet resistances are averages of at least four samples.

2.5 References

- (1) Neuvo, Y.; Ylönen, S. Bit Bang Rays to the Future. 286.
- (2) Tobjörk, D.; Österbacka, R. Paper Electronics. *Adv. Mater.* **2011**, *23* (17), 1935–1961. <https://doi.org/10.1002/adma.201004692>.
- (3) Zhang, Y.-Z.; Wang, Y.; Cheng, T.; Lai, W.-Y.; Pang, H.; Huang, W. Flexible Supercapacitors Based on Paper Substrates: A New Paradigm for Low-Cost Energy Storage. *Chem. Soc. Rev.* **2015**, *44* (15), 5181–5199. <https://doi.org/10.1039/C5CS00174A>.
- (4) Jung, Y. H.; Chang, T.-H.; Zhang, H.; Yao, C.; Zheng, Q.; Yang, V. W.; Mi, H.; Kim, M.; Cho, S. J.; Park, D.-W.; Jiang, H.; Lee, J.; Qiu, Y.; Zhou, W.; Cai, Z.; Gong, S.; Ma, Z. High-Performance Green Flexible Electronics Based on Biodegradable Cellulose Nanofibril Paper. *Nat. Commun.* **2015**, *6* (1), 7170. <https://doi.org/10.1038/ncomms8170>.
- (5) Kang, D. J.; González-García, L.; Kraus, T. Soft Electronics by Inkjet Printing Metal Inks on Porous Substrates. *Flex. Print. Electron.* **2022**, *7* (3), 033001. <https://doi.org/10.1088/2058-8585/ac8360>.

Chapter 2: Synchronizing the pore size of paper substrates
and aspect ratio of silver nanowires to improve printed electronics

- (6) Zhang, Y.; Zhang, T.; Huang, Z.; Yang, J. A New Class of Electronic Devices Based on Flexible Porous Substrates. *Adv. Sci.* **2022**, *9* (7), 2105084. <https://doi.org/10.1002/advs.202105084>.
- (7) Patil, P.; Patil, S.; Kate, P.; A. Kulkarni, A. Inkjet Printing of Silver Nanowires on Flexible Surfaces and Methodologies to Improve the Conductivity and Stability of the Printed Patterns. *Nanoscale Adv.* **2021**, *3* (1), 240–248. <https://doi.org/10.1039/D0NA00684J>.
- (8) Finn, D. J.; Lotya, M.; Coleman, J. N. Inkjet Printing of Silver Nanowire Networks. *ACS Appl. Mater. Interfaces* **2015**, *7* (17), 9254–9261. <https://doi.org/10.1021/acsami.5b01875>.
- (9) J. Scheideler, W.; Smith, J.; Deckman, I.; Chung, S.; Claudia Arias, A.; Subramanian, V. A Robust, Gravure-Printed, Silver Nanowire/Metal Oxide Hybrid Electrode for High-Throughput Patterned Transparent Conductors. *J. Mater. Chem. C* **2016**, *4* (15), 3248–3255. <https://doi.org/10.1039/C5TC04364F>.
- (10) Huang, Q.; Zhu, Y. Gravure Printing of Water-Based Silver Nanowire Ink on Plastic Substrate for Flexible Electronics. *Sci. Rep.* **2018**, *8* (1), 15167. <https://doi.org/10.1038/s41598-018-33494-9>.
- (11) Li, R.-Z.; Hu, A.; Zhang, T.; Oakes, K. D. Direct Writing on Paper of Foldable Capacitive Touch Pads with Silver Nanowire Inks. *ACS Appl. Mater. Interfaces* **2014**, *6* (23), 21721–21729. <https://doi.org/10.1021/am506987w>.
- (12) G. Nair, K.; Jayaseelan, D.; Biji, P. Direct-Writing of Circuit Interconnects on Cellulose Paper Using Ultra-Long, Silver Nanowires Based Conducting Ink. *RSC Adv.* **2015**, *5* (93), 76092–76100. <https://doi.org/10.1039/C5RA10837C>.

Chapter 2: Synchronizing the pore size of paper substrates
and aspect ratio of silver nanowires to improve printed electronics

- (13) Li, W.; Yang, S.; Shamim, A. Screen Printing of Silver Nanowires: Balancing Conductivity with Transparency While Maintaining Flexibility and Stretchability. *Npj Flex. Electron.* **2019**, *3* (1), 13. <https://doi.org/10.1038/s41528-019-0057-1>.
- (14) Lee, T.-W.; Lee, S.-E.; Jeong, Y. G. Highly Effective Electromagnetic Interference Shielding Materials Based on Silver Nanowire/Cellulose Papers. *ACS Appl. Mater. Interfaces* **2016**, *8* (20), 13123–13132. <https://doi.org/10.1021/acsami.6b02218>.
- (15) Zhan, Y.; Hao, X.; Wang, L.; Jiang, X.; Cheng, Y.; Wang, C.; Meng, Y.; Xia, H.; Chen, Z. Superhydrophobic and Flexible Silver Nanowire-Coated Cellulose Filter Papers with Sputter-Deposited Nickel Nanoparticles for Ultrahigh Electromagnetic Interference Shielding. *ACS Appl. Mater. Interfaces* **2021**, *13* (12), 14623–14633. <https://doi.org/10.1021/acsami.1c03692>.
- (16) Chen, Y.; Carmichael, R. S.; Carmichael, T. B. Patterned, Flexible, and Stretchable Silver Nanowire/Polymer Composite Films as Transparent Conductive Electrodes. *ACS Appl. Mater. Interfaces* **2019**, *11* (34), 31210–31219. <https://doi.org/10.1021/acsami.9b11149>.
- (17) Zhang, P.; Wyman, I.; Hu, J.; Lin, S.; Zhong, Z.; Tu, Y.; Huang, Z.; Wei, Y. Silver Nanowires: Synthesis Technologies, Growth Mechanism and Multifunctional Applications. *Mater. Sci. Eng. B* **2017**, *223*, 1–23. <https://doi.org/10.1016/j.mseb.2017.05.002>.
- (18) Langley, D.; Giusti, G.; Mayousse, C.; Celle, C.; Bellet, D.; Simonato, J.-P. Flexible Transparent Conductive Materials Based on Silver Nanowire Networks: A Review. *Nanotechnology* **2013**, *24* (45), 452001. <https://doi.org/10.1088/0957-4484/24/45/452001>.
- (19) Yao, S.; Zhu, Y. Wearable Multifunctional Sensors Using Printed Stretchable Conductors Made of Silver Nanowires. *Nanoscale* **2014**, *6* (4), 2345. <https://doi.org/10.1039/c3nr05496a>.

Chapter 2: Synchronizing the pore size of paper substrates
and aspect ratio of silver nanowires to improve printed electronics

- (20) Xu, X.; Zhou, J.; Jiang, L.; Lubineau, G.; Ng, T.; Ooi, B. S.; Liao, H.-Y.; Shen, C.; Chen, L.; Zhu, J. Y. Highly Transparent, Low-Haze, Hybrid Cellulose Nanopaper as Electrodes for Flexible Electronics. *Nanoscale* **2016**, *8* (24), 12294–12306. <https://doi.org/10.1039/C6NR02245F>.
- (21) Asadpoordarvish, A.; Sandström, A.; Larsen, C.; Bollström, R.; Toivakka, M.; Österbacka, R.; Edman, L. Light-Emitting Paper. *Adv. Funct. Mater.* **2015**, *25* (21), 3238–3245. <https://doi.org/10.1002/adfm.201500528>.
- (22) Shin, H.; Roh, J.; Song, J.; Roh, H.; Kang, C.; Lee, T.; Park, G.; An, K.; Kim, J. Y.; Kim, H.; Kwak, J.; Lee, C.; Kim, H. Highly Stable Organic Transistors on Paper Enabled by a Simple and Universal Surface Planarization Method. *Adv. Mater. Interfaces* **2019**, *6* (8), 1801731. <https://doi.org/10.1002/admi.201801731>.
- (23) Choi, J. O.; Jitsunari, F.; Asakawa, F.; Park, H. J.; Lee, D. S. Migration of Surrogate Contaminants in Paper and Paperboard into Water through Polyethylene Coating Layer. *Food Addit. Contam.* **2002**, *19* (12), 1200–1206. <https://doi.org/10.1080/02652030210151877>.
- (24) Cui, Z.; Han, Y.; Huang, Q.; Dong, J.; Zhu, Y. Electrohydrodynamic Printing of Silver Nanowires for Flexible and Stretchable Electronics. *Nanoscale* **2018**, *10* (15), 6806–6811. <https://doi.org/10.1039/C7NR09570H>.
- (25) Chen, Y.; Pang, L.; Li, Y.; Luo, H.; Duan, G.; Mei, C.; Xu, W.; Zhou, W.; Liu, K.; Jiang, S. Ultra-Thin and Highly Flexible Cellulose Nanofiber/Silver Nanowire Conductive Paper for Effective Electromagnetic Interference Shielding. *Compos. Part Appl. Sci. Manuf.* **2020**, *135*, 105960. <https://doi.org/10.1016/j.compositesa.2020.105960>.
- (26) Bergin, S. M.; Chen, Y.-H.; Rathmell, A. R.; Charbonneau, P.; Li, Z.-Y.; Wiley, B. J. The Effect of Nanowire Length and Diameter on the Properties of Transparent,

Chapter 2: Synchronizing the pore size of paper substrates
and aspect ratio of silver nanowires to improve printed electronics

Conducting Nanowire Films. *Nanoscale* **2012**, 4 (6), 1996.

<https://doi.org/10.1039/c2nr30126a>.

2.6 Supporting Information

Table S2.1 Drop diameter value for the AgNW front of a) AgNW30 and b) AgNW200. Data was taken from a 10 uL deposited onto filter paper and allowed to dry fully before diameter was measured.

a)

		Pore Size (μm)			
		2.5	8	11	20-25
Concentration (mg/mL)	0.4	8.2 ± 0.2 mm	7.6 ± 0.3 mm	6.9 ± 0.3 mm	6.6 ± 0.2 mm
	0.7	7.2 ± 0.3 mm	7.1 ± 0.3 mm	6.8 ± 0.2 mm	6.3 ± 0.1 mm
	2	7.2 ± 0.4 mm	6.9 ± 0.5 mm	6.6 ± 0.6 mm	6.7 ± 0.4 mm
	3	7.3 ± 0.2 mm	7.2 ± 0.7 mm	7.2 ± 0.3 mm	6.6 ± 0.3 mm

b)

		Pore Size (μm)			
		2.5	8	11	20-25
Concentration (mg/mL)	0.4	7.6 ± 0.5 mm	7.5 ± 0.3 mm	7.2 ± 0.1 mm	6.4 ± 0.3 mm
	0.7	7.5 ± 0.4 mm	7.5 ± 0.1 mm	7.3 ± 0.1 mm	6.3 ± 0.1 mm
	2	6.1 ± 0.2 mm	6.2 ± 0.3 mm	6.2 ± 0.3 mm	5.4 ± 0.1 mm
	3	6.1 ± 0.1 mm	5.9 ± 0.1 mm	5.6 ± 0.1 mm	5.1 ± 0.3 mm

CHAPTER 3
LIGHT-EMITTING PAPER FABRICATED USING DEBOSSSED CONTACT
PRINTING

3.1 Introduction

The seemingly ever-expanding system of the Internet of Things (IoT) propels the integration of printed electronic devices into many applications to gather and transmit data in and across many different fields.¹ Printed devices that are being created and incorporated into the IoT include printed sensors and antennas used for monitoring the quality of packages, pharmaceutical dose tracking, and more.¹ Among these devices there is a need for displays that are low cost and even disposable to convey information to the user. In smart packaging specifically, displays are important to enable the user to easily monitor the conditions of a product while in transport and storage.^{2,3} With perishable items, information on temperature, humidity, and atmospheric conditions gives insight into how fresh the contents are with displays relaying that data in real-time.⁴

At the same time, the growth of integrating electronic components into consumable products increases the burden of the already abundant electronic waste (e-waste) problem.⁵ Plastics remain the substrate of choice for printed electronics, polyethylene terephthalate (PET) specifically, due to its smoothness, flexibility, and low cost.⁶ However, they are not biodegradable and at the end of the device's lifecycle, the disposal process is harmful to the environment and human health.^{7,8} Paper is often looked at as a greener alternative as a substrate in printed electronics. It is abundant, biodegradable, and recyclable making it ideal for disposable electronics. Paper is also lightweight, flexible, and routinely used every day in different printing processes for graphics printing.^{9,10}

However, paper is composed of a network of hydrophilic cellulose fibers that create a porous structure and a rough surface.¹¹ This microstructure promotes wicking, making it challenging to print functional inks used in PE. Wicking disperses the functional ink, leading to problems with resolution and poor electrical performance.¹² There are approaches that try to combat this wicking, which include modifying the paper composition, planarizing the paper surface with a polymer layer, or patterning hydrophobic resists to guide ink deposition.^{10,13,14} Each of these methods adds steps to the fabrication process, increases the weight of the device, and the addition of polymer layers may also compromise the recyclability.

Our group previously published work on a resist-free alternative printing method for paper substrates that sidesteps all of these methods called Debossed Contact Printing (DCP).¹⁵ Here we build a multilayer light-emitting device on a paper substrate using DCP to pattern the substrate.

Paper electronics include sensors, antennas, transistors, diode structures, capacitors, and displays.⁹ With the attraction towards using paper as the substrate a few different types of light-emitting devices have been fabricated using different approaches. Light-Emitting Electrochemical Cells (LEECs) are simple light-emitting devices consisting of a bottom electrode, emissive material, and a transparent top electrode. Asadpoordarvish et al. built a LEEC on top of two different paper substrates by first adding a barrier layer or a top coating to planarize the rough paper surface. Using two different types of paper, one specialty paper and one low-cost copy paper, they demonstrated working LEECs on both substrates.¹⁶ The advantage of LEECs is their simple architecture, which makes them compatible with printing. However, the downside is their high sensitivity to environmental conditions, making them unreliable in applications such as smart packaging.

Organic Light Emitting Diodes (OLEDs) are an established light-emitting technology with a more complex architecture than that of LEECs. Yao et al. combined plastic and paper and used this mixture as a substrate for the fabrication of OLEDs. This approach combines benefits of both substrate materials, but the incorporation of plastic in the substrate may compromise the greenness of these devices.¹⁷ In addition, OLEDs require cathode materials with low work functions, which typically require vapor-based deposition methods. This requirement limits the ability to fabricate fully printed OLEDs.^{16,18}

Alternating Current Electroluminescent (ACEL) devices are a third type of light emitting technology that have been explored in lightweight, flexible, and stretchable electronics due to two advantages: their simple architecture and environmental stability. ACEL devices consist of an electroluminescent (EL) material sandwiched between two electrodes and emit light through a mechanism of field induced luminescence. The EL material, typically a zinc sulfide compound with a copper dopant, determines the colour

output. The impurity of the copper in the crystal lattice of zinc sulfide gives off a blue colored light when activated.^{16,17} If the dopant was a different element, such as aluminum or manganese, a different color light would emit.¹⁹ The color and intensity of light can be tuned by adjusting doping levels or changing the frequency.^{19,20}

Kim et al. created an ACEL device using four different paper substrates where a passivation layer is included in the fabrication to aid in planarizing the rough paper surface.²¹ As with other paper-based light-emitting devices, this reoccurring theme of planarizing the paper before building devices on the surface adds an extra step and compromises the recyclability of the paper substrate.

The Carmichael group recently created an alternative patterning approach for paper-based electronics that does not require any additional coatings or layers on the paper substrate.¹⁵ DCP is a resist-free printing method wherein we take advantage of the porosity of paper by selectively compressing the pores to create the pattern. DCP uses a debossing tip to apply pressure to the paper substrate. The pressure from the debossing tip collapses the pore structure, creating a relief pattern in the paper in a serial manner. When an unpatterned roller coated with a functional ink contacts the paper substrate, the ink transfers only to the raised regions of the relief pattern and not in the debossed trenches. The compressed pores in the trenches also act as a boundary to inhibit ink from wicking outside the printed pattern.¹⁵ We previously demonstrated that conductive inks such as carbon black ink, PEDOT: PSS ink, and silver (Ag) ink can be successfully used with this printing technique.

Applications that have been demonstrated using the DCP method include ultrahigh-frequency radio frequency identification (UHF RFID) tags and proximity sensing wallpaper. The UHF RFID tags were fabricated by debossing an antenna pattern into a paper substrate and applying a conductive silver ink. Cold soldering a microchip from a commercial tag to the antenna gave a functional UHF RFID tag with read/write capability.¹⁵ The second application is a patterned carbon black electrode used as a sample for proximity sensing smart wallpaper. This was connected to a bare conductive microcontroller that sensed a change in capacitance. It was demonstrated that this wallpaper could be used to turn a smart light on and off depending on the capacitance.¹⁵

These diverse applications show DCP is an effective, simple way to make single layer devices with a conductive pattern on paper. Here we further develop this method to make multilayered ACEL devices on paper.

3.2 Results and Discussion

Using the basic requirements for an ACEL device, we built up a multilayer ACEL device on a debossed paper substrate using roller printing to deposit all layers as illustrated in **Figure 3.1**. Fabrication of thin-film devices requires each layer to be uniform and pinhole-free. Pathways between the top and bottom electrodes cause device failure through shorting. In addition, it is essential to have uniform contact between the layers to enable the device to function properly. Therefore, we examined each printed layer using optical microscopy to evaluate the uniformity and examined the adhesion between layers.

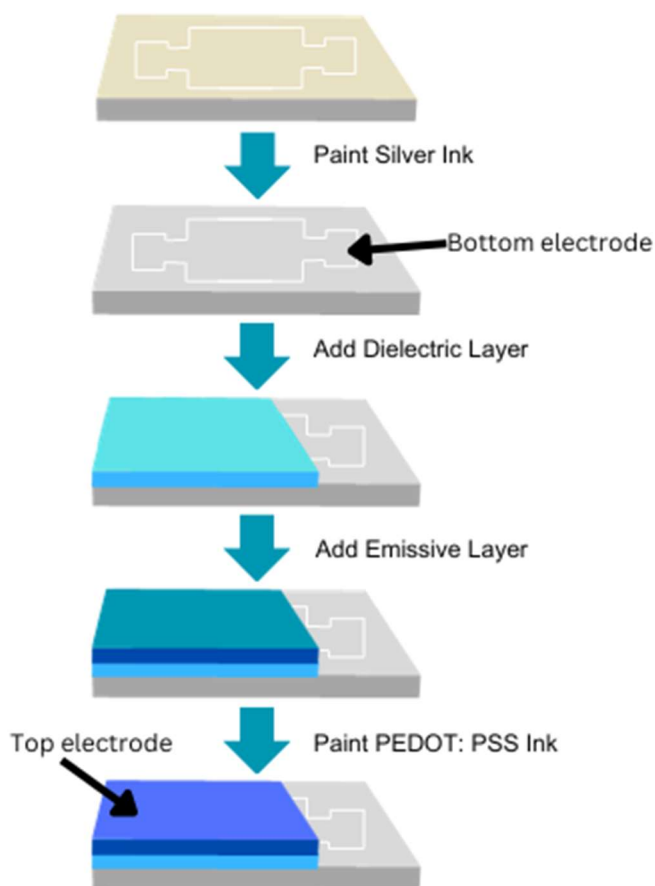


Figure 3.1 Schematic of paper-based ACEL device fabrication.

The fabrication scheme is depicted in Figure 3.1. We used a Cricut Maker equipped with a debossing tool to create the pattern on a watercolour paper substrate. We used the Cricket Design Space to design the pattern, which is shown in **Figure 3.2**. Three passes of the same design with the debossing tip result in indents of $\sim 100 \mu\text{m}$, which has been shown to be optimal to define the pattern with subsequent roller printing of functional inks. The design provides electrical contact to the top and bottom electrodes and a centre region for light emission.



Figure 3.2 Picture of debossed pattern on a paper substrate.

We used an unpatterned roller to print all layers on the device. Since thin films are often made by spincoating, we also used this method for comparison for printing the dielectric and emissive layers. When comparing the two methods, roller printing produced a layer with similar quality to that produced by spincoating (**Figure S3.1**). Roller printing is easily scalable for industry purposes and is known for its high speed and continuous production, making sense for its use within printed electronics.

We selected Ag paint as the bottom electrode due to its high conductivity and printability. Roller printing over the entire substrate deposited the silver ink only in the raised regions. The debossed pores remain free of ink and create a boundary to prevent the ink from spreading outside the debossed region. Conductivity measurements with the probes placed on the inside and outside of the debossed pattern showed no conductivity, indicating the debossed trench provides good pattern definition. The patterning done by this first layer of material sets the tone for the rest of the device buildup. The sheet resistance of the inside of the pattern with one coat of Ag paint was $1.2 \pm 0.7 \text{ } \Omega/\text{sq}$. Upon inspection under the microscope, however, the surface of the silver paint did not appear uniform (**Figure 3.2a**). Applying a second coat of silver paint provided better surface coverage and uniformity (**Figure 3.2b**), and reduced the sheet resistance to $0.2 \pm 0.1 \text{ } \Omega/\text{sq}$.

Next, we added a dielectric layer to aid in planarizing the silver electrode surface (**Figure S3.2**). This layer was composed of barium titanate dispersed in an elastomeric matrix and was printed to leave a portion of the bottom Ag electrode exposed for electrical contact (Figure 3.1). We explored several elastomer matrices, which included the two silicone elastomers Ecoflex and polydimethylsiloxane (PDMS) and a

polyurethane adhesive (Norland Optical Adhesive 73, NOA-73). We found that Ecoflex did not adhere well to the surface of the silver electrode, and among the other options, PDMS (**Figure 3.2c**) gave a more uniform layer compared to NOA-73.

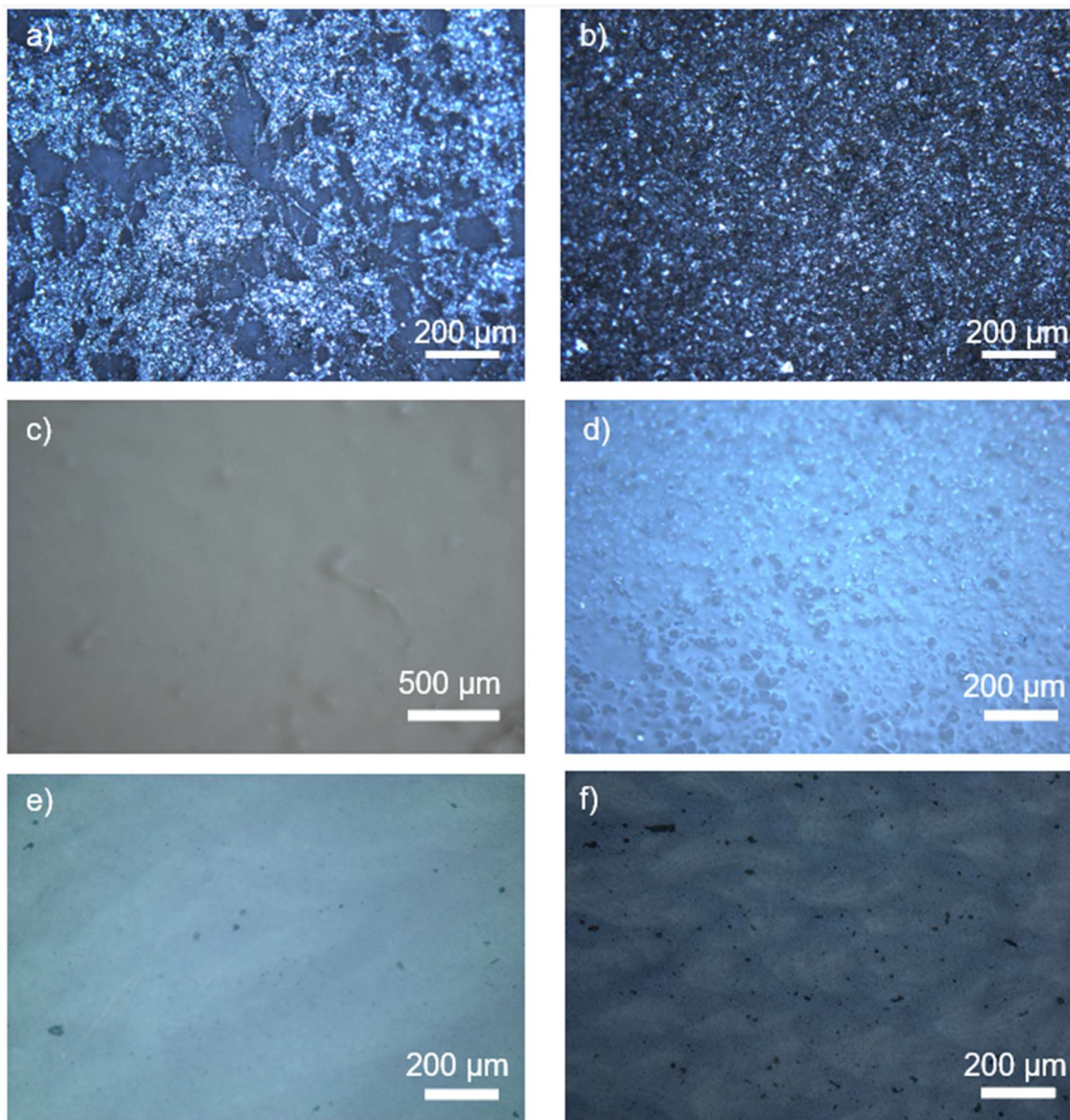


Figure 3.3 a) Microscope image of one coat of silver ink on paper, b) Microscope image of two coats of silver ink on paper, c) Microscope image of barium titanate mixed with PDMS layer d) Microscope image of copper doped zinc sulfide mixed with PDMS layer, e) Microscope image of 2 coats of PEDOT:PSS printed on top of PDMS, f) Microscope image of 2 coats of PEDOT:PSS printed on top of NOA-73.

After curing the PDMS-based dielectric layer, we printed the emissive layer, which contains the electroluminescent material. The emissive layer consisted of zinc sulfide particles doped with copper phosphor (ZnS:Cu) dispersed in a PDMS matrix. Using PDMS for both the dielectric and emissive layers ensured robust contact through PDMS-PDMS crosslinking between the layers. Optical micrographs of the emissive layer show the copper-doped zinc sulfide particles embedded in PDMS (**Figure 3.2d**).

Finally, we used PEDOT: PSS as the top electrode. PEDOT:PSS is a conductive and transparent polymer that permits light emission from the device. For printability, the PEDOT:PSS ink used for the top electrode must wet and adhere to the emissive layer surface. Contact angle measurements at this stage of the device buildup provided an understanding of the interface between the emissive layer and the top transparent electrode. By nature, PDMS is hydrophobic with a water contact angle of 112° .²² The water contact angle of the emissive layer was similar to this value ($110.9 \pm 6.4^\circ$).

A big factor in getting subsequent layers to print and adhere to the previous one is the wettability of the ink on the substrate.²³ Inks typically contain a polar solvent that will wet onto surfaces that are hydrophilic since the ink droplets are attracted to the substrate. The inks have an easier time spread uniformly, giving an even layer.¹⁴ The advantage of using PDMS as the matrix for the emissive layer is that the surface of PDMS can be oxidized to generate a thin, hydrophilic SiO₂ layer on the surface.²⁴ We used ultra-violet (UV) ozone treatment to oxidize the surface of the emissive layer, which reduced the water contact angle to $75.5 \pm 8.4^\circ$.

We printed two coats of PEDOT: PSS ink on this surface, which produced a uniform layer with a sheet resistance value of $111.6 \pm 31.8 \Omega/\text{sq}$. This value is much lower than when two coats of PEDOT: PSS are printed on paper alone, which has been reported at $10000 \pm 2000 \Omega/\text{sq}$.¹⁵ We tried using three coats of PEDOT: PSS to lower the sheet resistance of that layer, which it was reduced, but there appeared no visible benefit with the light emission when testing the device and the extra coat added unnecessary weight onto the device. As mentioned above, we ultimately chose PDMS over NOA-73 as the elastomer matrix for the phosphor particles. **Figure 3.2e-f** solidifies this choice as a more consistent and uniform PEDOT: PSS layer is achieved when printed on PDMS (Figure

3.2e) than when it is printed on NOA-73 (Figure 3.2f). This translated to more uniform light emission when testing the devices.

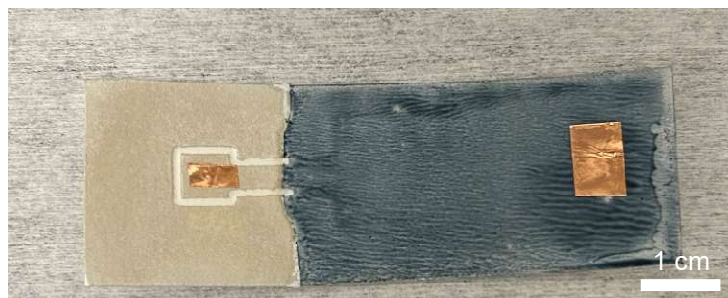


Figure 3.4 Photograph of the completed ACEL device with copper tape as bottom and top contact.

The finished device is pictured in **Figure 3.4**, showing the silver bottom electrode on the left and the PEDOT:PSS transparent top electrode on the right. We used copper tape to make electrical contact to the two electrodes. We tested the ACEL devices at 500 V AC with a frequency of 2 kHz, which produced fairly uniform blue light emission (**Figure 3.5**). The uniformity of the light emission can be improved by careful optimization of the device layers to improve uniformity and adhesion of the layers. Brightness variation can also be caused by the roughness of the electrodes, which lead to inconsistent electric fields during operation of the device.

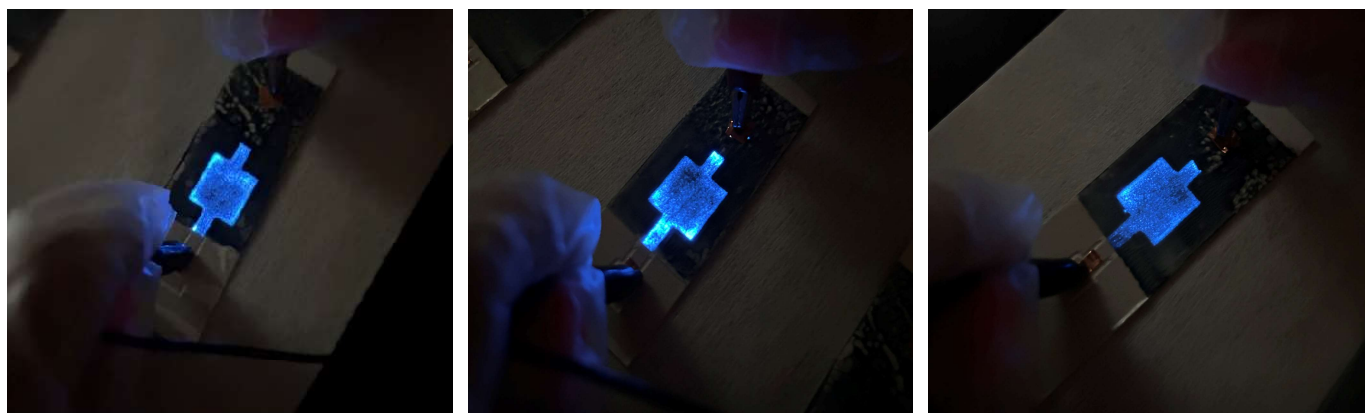


Figure 3.5 Photograph of three ACEL devices when subjected to AC voltage.

3.3 Conclusion

In conclusion, we successfully achieved light emission with our multilayer paper-based ACEL devices composed of silver ink and PEDOT: PSS as the electrodes and

copper doped zinc sulfide phosphor particles as the EL material. In the future, this project can be progressed by quantifying the light emission using an optometer with an integrating sphere. To enhance its suitability for flexible device applications the performance when subjected to bending strains should be explored. The promising results of using DCP to fabricate multilayered ACEL devices opens the possibility to explore more complex and intricate patterns or patterning different layers of the device.

3.4 Experimental

Materials: The paper used is a 300 g/m² watercolor paper obtained from Artist's Loft (Irving, TX). The non-volatile organic content (VOC) silver ink was obtained from SPI supplies (West Chester, PA) and used as received. The copper-doped zinc sulfide phosphor particles were obtained by KPT and used as received. The Sylgard 184 or polydimethyl siloxane (PDMS) was obtained from and used as received. The PEDOT: PSS ink was obtained from Sigma-Aldrich and used as received.

Preparation of Debossed Paper Substrate: A Cricut Maker equipped with a debossing tip was used to deboss patterns on the paper substrates. Digital designs were prepared directly in the Cricut Design Space. Debossing was done using the "heavy watercolor paper 140 lb" setting at a "regular pressure" in the Cricut Design Space. The samples were debossed with 3 passes to create a final imprint ~ 100 μm deep.

Electroluminescent Device Fabrication: Samples were roller printed with silver ink and annealed on a hot plate at 60°C for 20 minutes. Next PDMS was made by mixing 10:1 w:w ratio of elastomer base to curing agent. A dielectric material, barium titanate was added in a 1:1 w:w ratio of uncured PDMS and barium titanate. This mixture was degassed for five minutes in a desiccator, roller printed, and put in a 60°C oven overnight to cure. The following day, the same process was done with PDMS and copper-doped zinc sulfide phosphor where they were mixed in a 1:1 by w:w ratio, degassed for 5 minutes, roller printed, and put in a 60°C oven overnight to cure. Samples were then oxidized in UV ozone for 20 minutes before adding PEDOT: PSS ink by roller printing. Two layers of PEDOT: PSS ink were applied with samples being dried overnight in a 60°C oven after each layer.

Characterization: Optical images were taken using an Olympus BX51 microscope and Olympus Q-Color3 digital camera. Sheet resistances of 1 cm² samples were measured with a Keithly 2601 A Sourcemeter. The reported sheet resistance is an average of at least 4 samples. Contact angle measurements were taken using an Rame-Hart contact angle goniometer.

Device Testing: Paper-based ACEL devices were tested at 500 V AC with a frequency of 2 kHz that was inverted from 3 V DC from a Keithly 2601 A Sourcemeter using an inverter (Sparkfun).

3.5 References

- (1) Bakar, K. B. A.; Zuhra, F. T.; Isyaku, B.; Sulaiman, S. B. A Review on the Immediate Advancement of the Internet of Things in Wireless Telecommunications. *IEEE Access* **2023**, *11*, 21020–21048. <https://doi.org/10.1109/ACCESS.2023.3250466>.
- (2) Realini, C. E.; Marcos, B. Active and Intelligent Packaging Systems for a Modern Society. *Meat Sci.* **2014**, *98* (3), 404–419. <https://doi.org/10.1016/j.meatsci.2014.06.031>.
- (3) Kang, H.; Park, H.; Park, Y.; Jung, M.; Kim, B. C.; Wallace, G.; Cho, G. Fully Roll-to-Roll Gravure Printable Wireless (13.56 MHz) Sensor-Signage Tags for Smart Packaging. *Sci. Rep.*
- (4) Schaefer, D.; Cheung, W. M. Smart Packaging: Opportunities and Challenges. *Procedia CIRP* **2018**, *72*, 1022–1027. <https://doi.org/10.1016/j.procir.2018.03.240>.
- (5) Habib, K.; Mohammadi, E.; Vihanga Withanage, S. A First Comprehensive Estimate of Electronic Waste in Canada. *J. Hazard. Mater.* **2023**, *448*, 130865. <https://doi.org/10.1016/j.jhazmat.2023.130865>.
- (6) Chang, J. S.; Facchetti, A. F.; Reuss, R. A Circuits and Systems Perspective of Organic/Printed Electronics: Review, Challenges, and Contemporary and Emerging Design Approaches. *IEEE J. Emerg. Sel. Top. Circuits Syst.* **2017**, *7* (1), 7–26. <https://doi.org/10.1109/JETCAS.2017.2673863>.
- (7) Geyer, R.; Jambeck, J. R.; Law, K. L. Production, Use, and Fate of All Plastics Ever Made. *Sci. Adv.* **2017**, *3* (7), e1700782. <https://doi.org/10.1126/sciadv.1700782>.

- (8) Riechers, M.; Fanini, L.; Apicella, A.; Galván, C. B.; Blondel, E.; Espiña, B.; Kefer, S.; Keroullé, T.; Klun, K.; Pereira, T. R.; Ronchi, F.; Rodríguez, P. R.; Sardon, H.; Silva, A. V.; Stulgis, M.; Ibarra-González, N. Plastics in Our Ocean as Transdisciplinary Challenge. *Mar. Pollut. Bull.* **2021**, *164*, 112051. <https://doi.org/10.1016/j.marpolbul.2021.112051>.
- (9) Tobjörk, D.; Österbacka, R. Paper Electronics. *Adv. Mater.* **2011**, *23* (17), 1935–1961. <https://doi.org/10.1002/adma.201004692>.
- (10) Jansson, E.; Lyytikäinen, J.; Tanninen, P.; Eiroma, K.; Leminen, V.; Immonen, K.; Hakola, L. Suitability of Paper-Based Substrates for Printed Electronics. *Materials* **2022**, *15* (3), 957. <https://doi.org/10.3390/ma15030957>.
- (11) Khan, S. M.; Nassar, J. M.; Hussain, M. M. Paper as a Substrate and an Active Material in Paper Electronics. *ACS Appl. Electron. Mater.* **2021**, *3* (1), 30–52. <https://doi.org/10.1021/acsaelm.0c00484>.
- (12) Cao, L.; Bai, X.; Lin, Z.; Zhang, P.; Deng, S.; Du, X.; Li, W. The Preparation of Ag Nanoparticle and Ink Used for Inkjet Printing of Paper Based Conductive Patterns. *Materials* **2017**, *10* (9), 1004. <https://doi.org/10.3390/ma10091004>.
- (13) Ahn, E.; Kim, T.; Jeon, Y.; Kim, B.-S. A4 Paper Chemistry: Synthesis of a Versatile and Chemically Modifiable Cellulose Membrane. *ACS Nano* **2020**, *14* (5), 6173–6180. <https://doi.org/10.1021/acsnano.0c02211>.
- (14) Tian, D.; Song, Y.; Jiang, L. Patterning of Controllable Surface Wettability for Printing Techniques. *Chem. Soc. Rev.* **2013**, *42* (12), 5184. <https://doi.org/10.1039/c3cs35501b>.
- (15) Mechael, S. S.; D’Amaral, G. M.; Carmichael, T. B. Debossed Contact Printing as a Patterning Method for Paper-Based Electronics.
- (16) Asadpoordarvish, A.; Sandström, A.; Larsen, C.; Bollström, R.; Toivakka, M.; Österbacka, R.; Edman, L. Light-Emitting Paper. *Adv. Funct. Mater.* **2015**, *25* (21), 3238–3245. <https://doi.org/10.1002/adfm.201500528>.
- (17) Yao, Y.; Tao, J.; Zou, J.; Zhang, B.; Li, T.; Dai, J.; Zhu, M.; Wang, S.; Fu, K. K.; Henderson, D.; Hitz, E.; Peng, J.; Hu, L. Light Management in Plastic–Paper Hybrid

- Substrate towards High-Performance Optoelectronics. *Energy Environ. Sci.* **2016**, *9* (7), 2278–2285. <https://doi.org/10.1039/C6EE01011C>.
- (18) Yoon, D.-Y.; Moon, D.-G. Bright Flexible Organic Light-Emitting Devices on Copy Paper Substrates. *Curr. Appl. Phys.* **2012**, *12*, e29–e32. <https://doi.org/10.1016/j.cap.2011.04.033>.
- (19) Deng, Z.; Tong, L.; Flores, M.; Lin, S.; Cheng, J.-X.; Yan, H.; Liu, Y. High-Quality Manganese-Doped Zinc Sulfide Quantum Rods with Tunable Dual-Color and Multiphoton Emissions. *J. Am. Chem. Soc.* **2011**, *133* (14), 5389–5396. <https://doi.org/10.1021/ja110996c>.
- (20) Park, N.-M.; Koo, J. B.; Oh, J.-Y.; Kim, H. J.; Park, C. W.; Ahn, S.-D.; Jung, S. W. Electroluminescent Nanocellulose Paper. *Mater. Lett.* **2017**, *196*, 12–15. <https://doi.org/10.1016/j.matlet.2017.03.003>.
- (21) Kim, J.-Y.; Park, S. H.; Jeong, T.; Bae, M. J.; Song, S.; Lee, J.; Han, I. T.; Jung, D.; Yu, S. Paper as a Substrate for Inorganic Powder Electroluminescence Devices. *IEEE Trans. Electron Devices* **2010**, *57* (6), 1470–1474. <https://doi.org/10.1109/TED.2010.2045675>.

3.6 Supporting Information

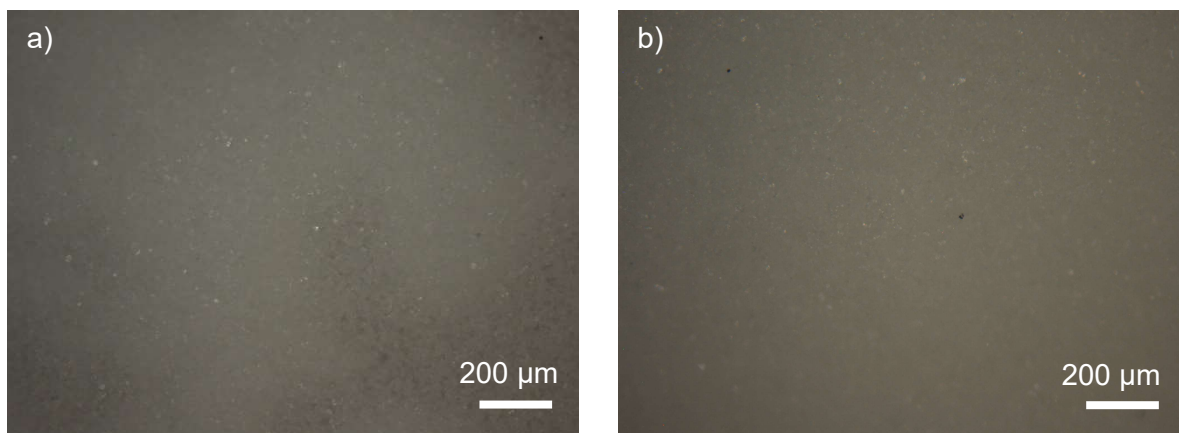


Figure S3.1 Microscope images of the dielectric layer when a) spincoated, and b) roller printed.

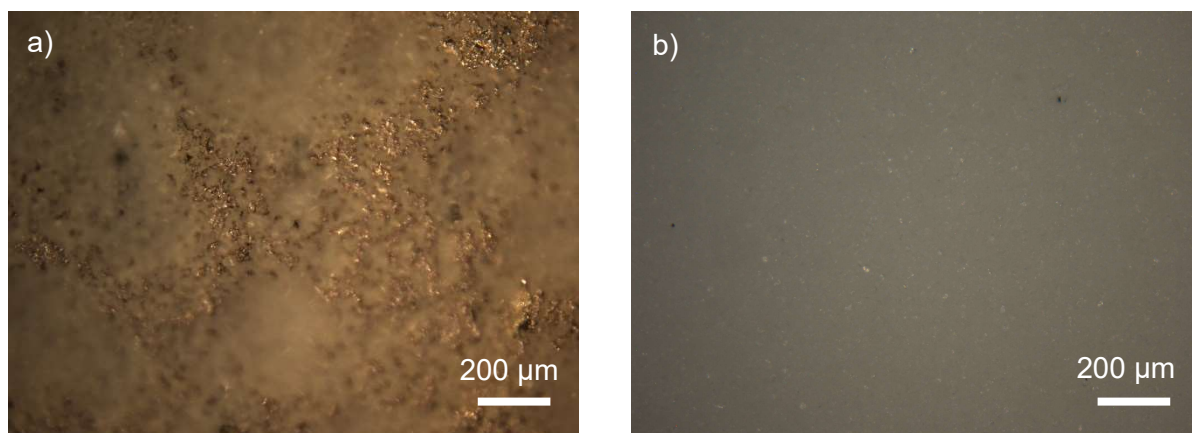


Figure S3.2 Microscope images of the emissive layer with a) no dielectric layer, and b) with barium titanate as the dielectric layer.

CHAPTER 4
CONCLUSION AND OUTLOOK

The major goal of this thesis was to bridge the literature gap of how ink interacts with paper and what parameters should be considered when selecting materials for printing. Considering the structure of the paper, we were able to show that the pore size of the paper is important and has an influence on the conductivity of a 1D nanomaterial active ink when printing. The knowledge of printing and its relationship to the structure of the paper will guide the selection of material in the future. We show it is possible to match the length of the AgNW inks and the paper pore size to help minimize wicking. Based on what kind of material is chosen, you can tune the sheet resistance for what is needed for the desired application. If the application requires a lower sheet resistance, then it would be recommended that a paper with a smaller pore size is used with a longer AgNW solution. If sheet resistance is not an important factor, then there is less limitation on what materials can be opted for. It is probable that these findings would extend to other 1D nanomaterials such as other metal NWs or carbon nanotubes (CNTs).

With the understanding that pore size has an effect on how inks wick during printing, this transitioned into looking at the process of DCP as a method for making devices. Manipulating the pore size by collapsing them allowed for a boundary to be made. This boundary can be made into virtually any design for potential display applications.

DCP is a promising printing method for paper-based printing electronics. With DCP, there is no need for resists or planarization of the paper substrate making it a more green and less wasteful process in comparison to existing methods discussed in this thesis. To make it useful beyond antennas, we need to be able to make multilayered devices. This thesis demonstrated that the device build-up process using this printing method is a simple and effective way to create multilayered devices. By characterizing each layer, we were able to successfully build an ACEL device on paper.

Looking into the future, this work can be continued by exploring different patterns, or combining sequential debossing and deposition steps to fabricate more complex devices, characterizing the light emission, and exploring how performance is affected by bending strain.

APPENDICES

9/13/23, 10:10 PM

Rightslink® by Copyright Clearance Center



Home



Help ▾



Live Chat



Sign in



Create Account

Debossed Contact Printing as a Patterning Method for Paper-Based Electronics



Author: Sara S. Mechael, Glória M. D'Amaral, Trícia Breen Carmichael

Publication: Applied Materials

Publisher: American Chemical Society

Date: Sep 1, 2023

Copyright © 2023, American Chemical Society

PERMISSION/LICENSE IS GRANTED FOR YOUR ORDER AT NO CHARGE

This type of permission/license, instead of the standard Terms and Conditions, is sent to you because no fee is being charged for your order. Please note the following:

- Permission is granted for your request in both print and electronic formats, and translations.
- If figures and/or tables were requested, they may be adapted or used in part.
- Please print this page for your records and send a copy of it to your publisher/graduate school.
- Appropriate credit for the requested material should be given as follows: "Reprinted (adapted) with permission from (COMPLETE REFERENCE CITATION), Copyright (YEAR) American Chemical Society." Insert appropriate information in place of the capitalized words.
- One-time permission is granted only for the use specified in your RightsLink request. No additional uses are granted (such as derivative works or other editions). For any uses, please submit a new request.

If credit is given to another source for the material you requested from RightsLink, permission must be obtained from that source.

[BACK](#)

[CLOSE WINDOW](#)



Screen printing of flexible piezoelectric based device on polyethylene terephthalate (PET) and paper for touch and force sensing applications

Author: Sepehr Emamian, Binu Baby Narakathu, Amer Abdulmahdi Chlaihawi, Bradley J. Bazuin, Massood Zandi Atashbar

Publication: Sensors and Actuators A: Physical

Publisher: Elsevier

Date: 15 August 2017

© 2017 Elsevier B.V. All rights reserved.

Order Completed

Thank you for your order.

This Agreement between University of Windsor -- Lauren Renaud ("You") and Elsevier ("Elsevier") consists of your license details and the terms and conditions provided by Elsevier and Copyright Clearance Center.

Your confirmation email will contain your order number for future reference.

License Number 5646761175866

[Printable Details](#)

License date Oct 12, 2023

SPRINGER NATURE LICENSE
TERMS AND CONDITIONS

Sep 17, 2023

This Agreement between University of Windsor -- Lauren Renaud ("You") and Springer Nature ("Springer Nature") consists of your license details and the terms and conditions provided by Springer Nature and Copyright Clearance Center.

License Number	5627970855985
License date	Sep 14, 2023
Licensed Content Publisher	Springer Nature
Licensed Content Publication	Nature Materials
Licensed Content Title	Flexible organic transistors and circuits with extreme bending stability
Licensed Content Author	Tsuyoshi Sekitani et al
Licensed Content Date	Nov 7, 2010
Type of Use	Thesis/Dissertation
Requestor type	academic/university or research institute
Format	print and electronic
Portion	figures/tables/illustrations
Number of figures/tables/illustrations	1

AIP PUBLISHING LICENSE
TERMS AND CONDITIONS

Sep 13, 2023

This Agreement between Univeristy of Windsor – Lauren Renaud ("You") and AIP Publishing ("AIP Publishing") consists of your license details and the terms and conditions provided by AIP Publishing and Copyright Clearance Center.

License Number	5627390802428
License date	Sep 13, 2023
Licensed Content Publisher	AIP Publishing
Licensed Content Publication	Biomicrofluidics
Licensed Content Title	Inkjet printed silver electrodes on macroporous paper for a paper-based isoelectric focusing device
Licensed Content Author	Gaspar, Cristina; Sikanen, Tiina
Licensed Content Date	Dec 28, 2016
Licensed Content Volume	10
Licensed Content Issue	6
Type of Use	Thesis/Dissertation
Requestor type	Author (original article)
Format	Print and electronic

This is a License Agreement between Lauren Renaud ("User") and Copyright Clearance Center, Inc. ("CCC") on behalf of the Rightsholder identified in the order details below. The license consists of the order details, the Marketplace Permissions General Terms and Conditions below, and any Rightsholder Terms and Conditions which are included below. All payments must be made in full to CCC in accordance with the Marketplace Permissions General Terms and Conditions below.

Order Date	13-Sep-2023	Type of Use	Republish in a thesis/dissertation
Order License ID	1396528-1	Publisher	Royal Society of Chemistry
ISSN	2050-7534	Portion	Image/photo/illustration

LICENSED CONTENT

Publication Title	Journal of materials chemistry. C, Materials for optical and electronic devices	Rightsholder	Royal Society of Chemistry
Article Title	Electrical functionality of inkjet-printed silver nanoparticle conductive tracks on nanostructured paper compared with those on plastic substrates	Publication Type	e-Journal
Author/Editor	Royal Society of Chemistry (Great Britain)	Start Page	5235
Date	01/01/2013	Issue	34
Language	English	Volume	1
Country	United Kingdom of Great Britain and Northern Ireland	URL	http://pubs.rsc.org/en/journals/journaliss...

This is a License Agreement between Lauren Renaud ("User") and Copyright Clearance Center, Inc. ("CCC") on behalf of the Rightsholder identified in the order details below. The license consists of the order details, the Marketplace Permissions General Terms and Conditions below, and any Rightsholder Terms and Conditions which are included below. All payments must be made in full to CCC in accordance with the Marketplace Permissions General Terms and Conditions below.

Order Date	13-Sep-2023	Type of Use	Republish in a thesis/dissertation
Order License ID	1396530-1	Publisher	IOP Publishing
ISSN	0957-4484	Portion	Chart/graph/table/figure

LICENSED CONTENT

Publication Title	Nanotechnology	Country	United Kingdom of Great Britain and Northern Ireland
Author/Editor	Institute of Physics (Great Britain)	Rightsholder	IOP Publishing, Ltd
Date	01/01/1990	Publication Type	Journal
Language	English		

REQUEST DETAILS

Portion Type	Chart/graph/table/figure	Distribution	Canada
Number of Charts / Graphs / Tables / Figures Requested	1	Translation	Original language of publication
Format (select all that apply)	Print, Electronic	Copies for the Disabled?	No
Who Will Republish the Content?	Academic institution	Minor Editing Privileges?	No
Duration of Use	Life of current and all future editions	Incidental Promotional Use?	No
Lifetime Unit Quantity	Up to 499	Currency	CAD
Rights Requested	Main product		

JOHN WILEY AND SONS LICENSE
TERMS AND CONDITIONS

Sep 17, 2023

This Agreement between Univeristy of Windsor -- Lauren Renaud ("You") and John Wiley and Sons ("John Wiley and Sons") consists of your license details and the terms and conditions provided by John Wiley and Sons and Copyright Clearance Center.

License Number	5627391405413
License date	Sep 13, 2023
Licensed Content Publisher	John Wiley and Sons
Licensed Content Publication	Advanced Optical Materials
Licensed Content Title	Advances in Alternating Current Electroluminescent Devices
Licensed Content Author	Handong Sun, Haoshuang Gu, Lian Xiao, et al
Licensed Content Date	Jan 23, 2019

VITA AUCTORIS

NAME: Lauren J. Renaud

PLACE OF BIRTH: Windsor, ON

YEAR OF BIRTH: 1999

EDUCATION: St. Thomas of Villanova High School, LaSalle, ON,
2017

University of Windsor, B.Sc., Windsor, ON, 2021

University of Windsor, M.Sc., Windsor, ON, 2023